



# FIRSTPASS SYSTEM SUCCESS

APPLICATION WORKSHOPS FOR HIGH-PERFORMANCE ELECTRONIC DESIGN



## Left-Handed Metamaterials for Microwave Engineering Applications

Author: Anthony Lai

Advisor: Prof. Tatsuo Itoh

*Department of Electrical Engineering  
UCLA*

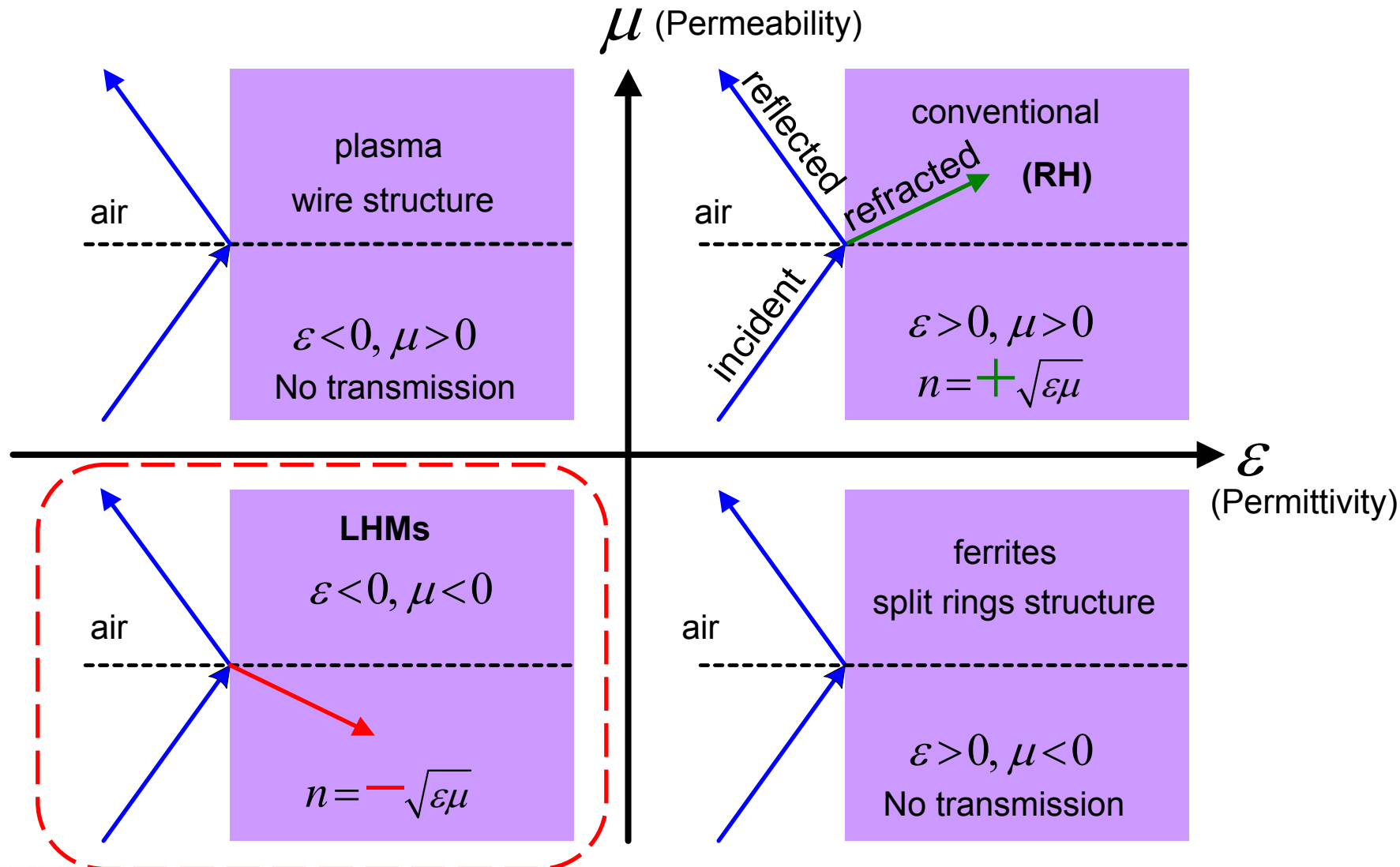


# Outline

- Left-Handed Metamaterial Introduction
  - ❖ Resonant approach
  - ❖ Transmission line approach
- Composite Right/Left-Handed Metamaterial
- Metamaterial-Based Microwave Devices
  - ❖ Dominant leaky-wave antenna
  - ❖ Small, resonant backward wave antennas
  - ❖ Dual-band hybrid coupler
  - ❖ Negative refractive index flat lens
- Future Trends
- Summary



# What is a Left-Handed Metamaterial?



1967: Veselago speculates about the possibility of LHMs and discusses their properties.

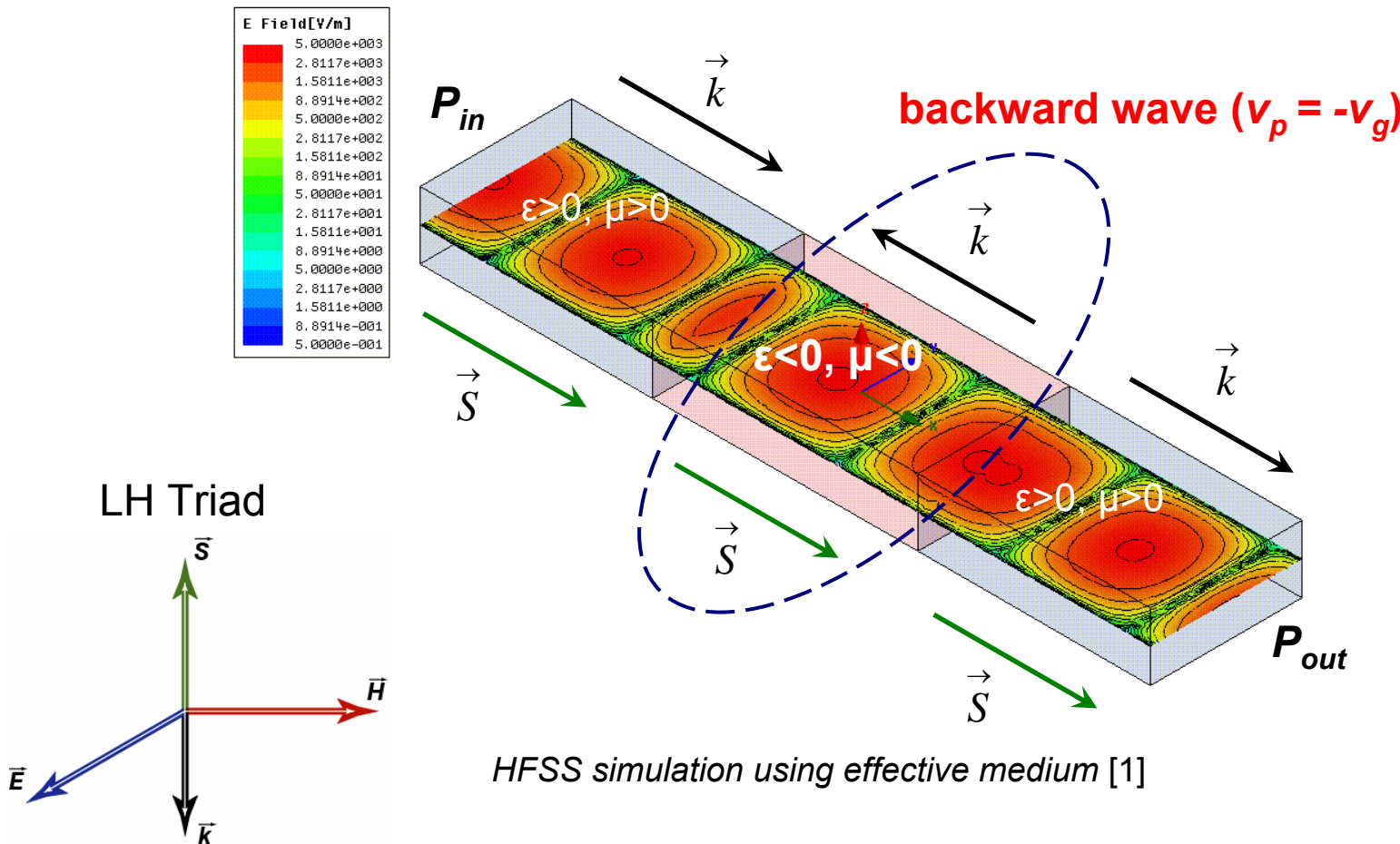
# What is a Left-Handed Metamaterial?

## Veselago's Conclusions

- Simultaneous negative permittivity ( $-\epsilon$ ) and permeability ( $-\mu$ ).
- Reversal of Snell's Law (negative index of refraction), Doppler Effect, and Cerenkov Effect.
- Electric field, Magnetic field, and Wavevector of electromagnetic wave in a LHM form a left-handed triad.
- LHMs support **backward waves**: anti-parallel group and phase velocity.
- Artificial effectively homogenous structure: metamaterial.



# Rectangular Waveguide Filled with LHM

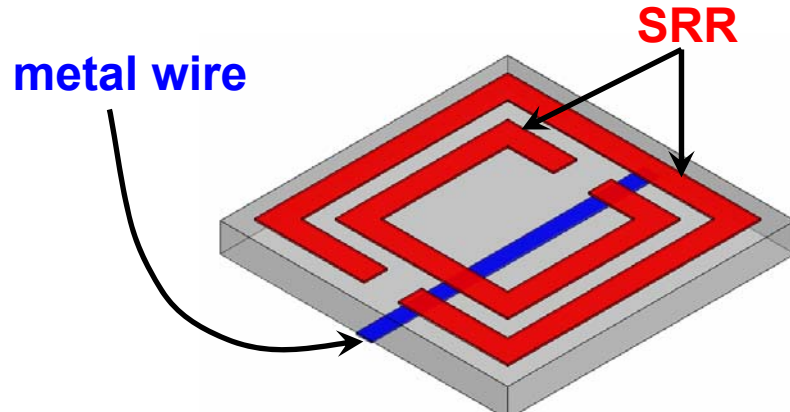


naturally occurring LH material has not yet been discovered

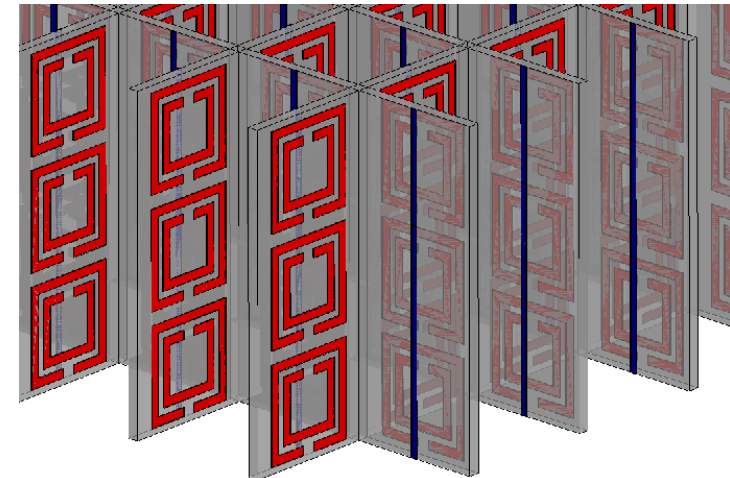


# LHM – Resonant Approach

- 1967: LHM were first proposed by Russian Physicist Victor Veselago
- 2001: LHM realized based on split ring resonators - **Resonant Approach** towards LHM [2].



SRR-based LHM unit-cell



**SRR**: at **resonance** provides  $\mu < 0$

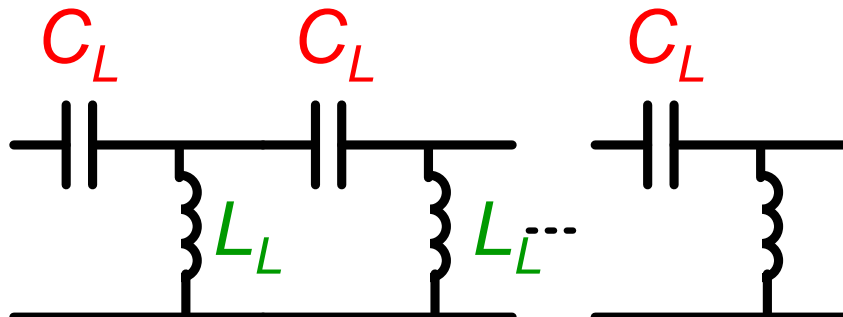
**metal wire**: provides  $\epsilon < 0$

- SRR-based metamaterials only exhibit LH properties at **resonance** - inherently **narrow-band** and **lossy**.
- SRR-based LHM are bulky - not practical for microwave engineering applications.



# LHM – Transmission Line Approach

- Backward wave transmission line can form a non-resonant LHM [3]-[4].
- **Transmission Line Approach** is based on the dual of a conventional transmission line.



*Perfect LH transmission line*

**Series capacitance ( $C_L$ ) and shunt inductance ( $L_L$ ) combination supports a fundamental backward wave.**

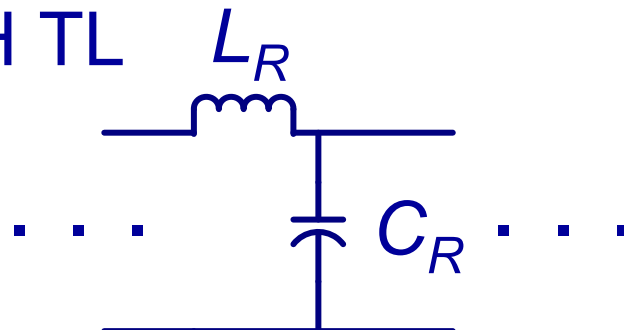
$$\beta = \frac{-1}{\omega \sqrt{C_L L_L}}$$

- Perfect LH transmission line not resonant dependent - low-loss and broad-band performance.
- However, perfect LH transmission line is not possible due to unavoidable **parasitic right-handed (RH) effects** occurring with physical realization.

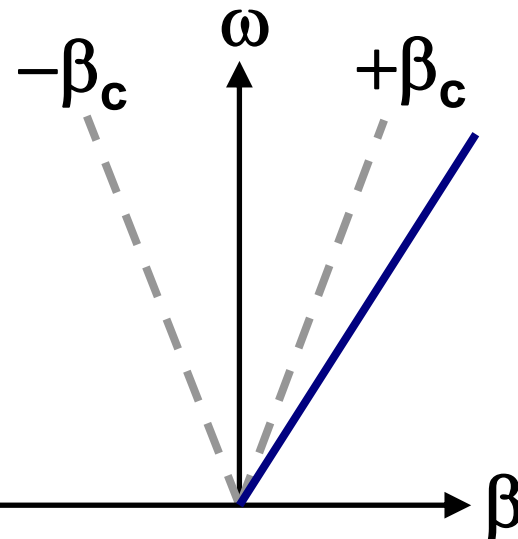


# Transmission Line Approach

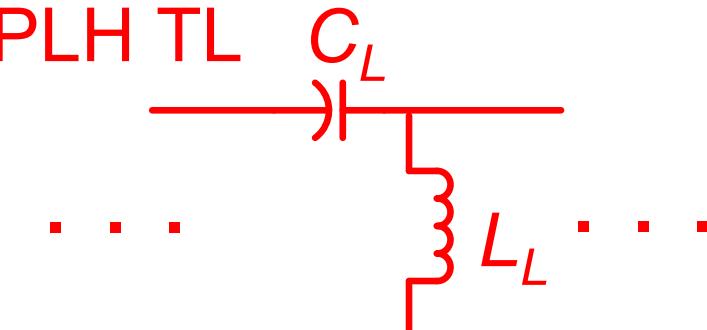
PRH TL



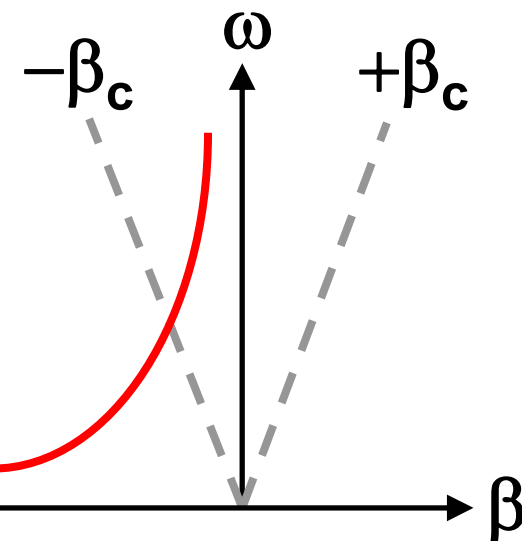
$$\beta_{PRH} = \omega \sqrt{C_R L_R}$$



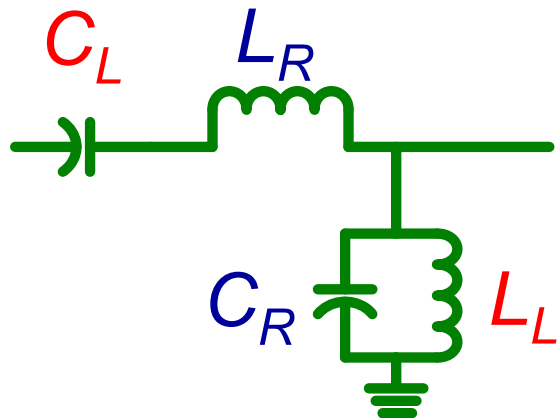
PLH TL



$$\beta_{PLH} = -\frac{1}{\omega \sqrt{C_L L_L}}$$



# Composite Right/Left-Handed Metamaterial

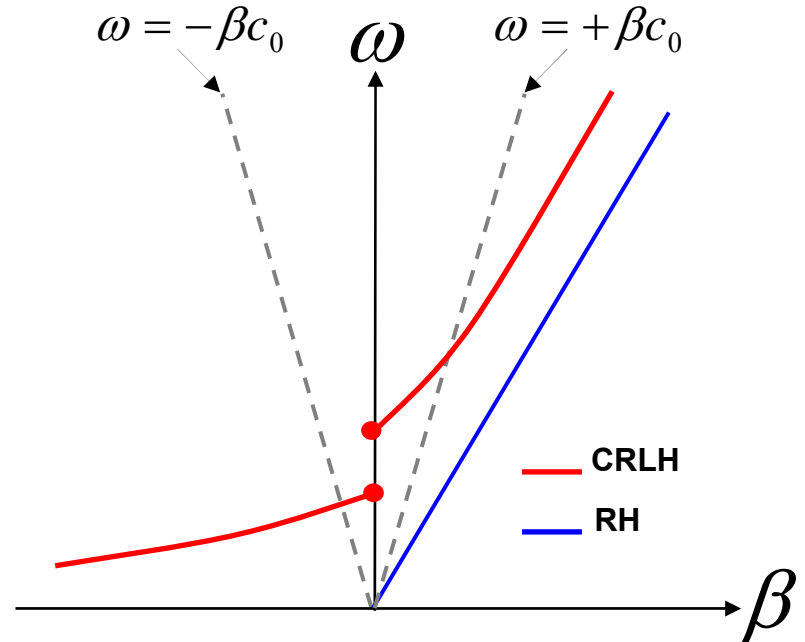


$$\beta = s(\omega) \sqrt{\omega^2 C_R L_R + \frac{1}{\omega^2 C_L L_L} - \left( \frac{L_R}{L_L} + \frac{C_R}{C_L} \right)},$$

$$s(\omega) = \begin{cases} -1 & \text{if } \omega < \min(\omega_{se}, \omega_{sh}) \\ +1 & \text{if } \omega > \max(\omega_{se}, \omega_{sh}) \end{cases},$$

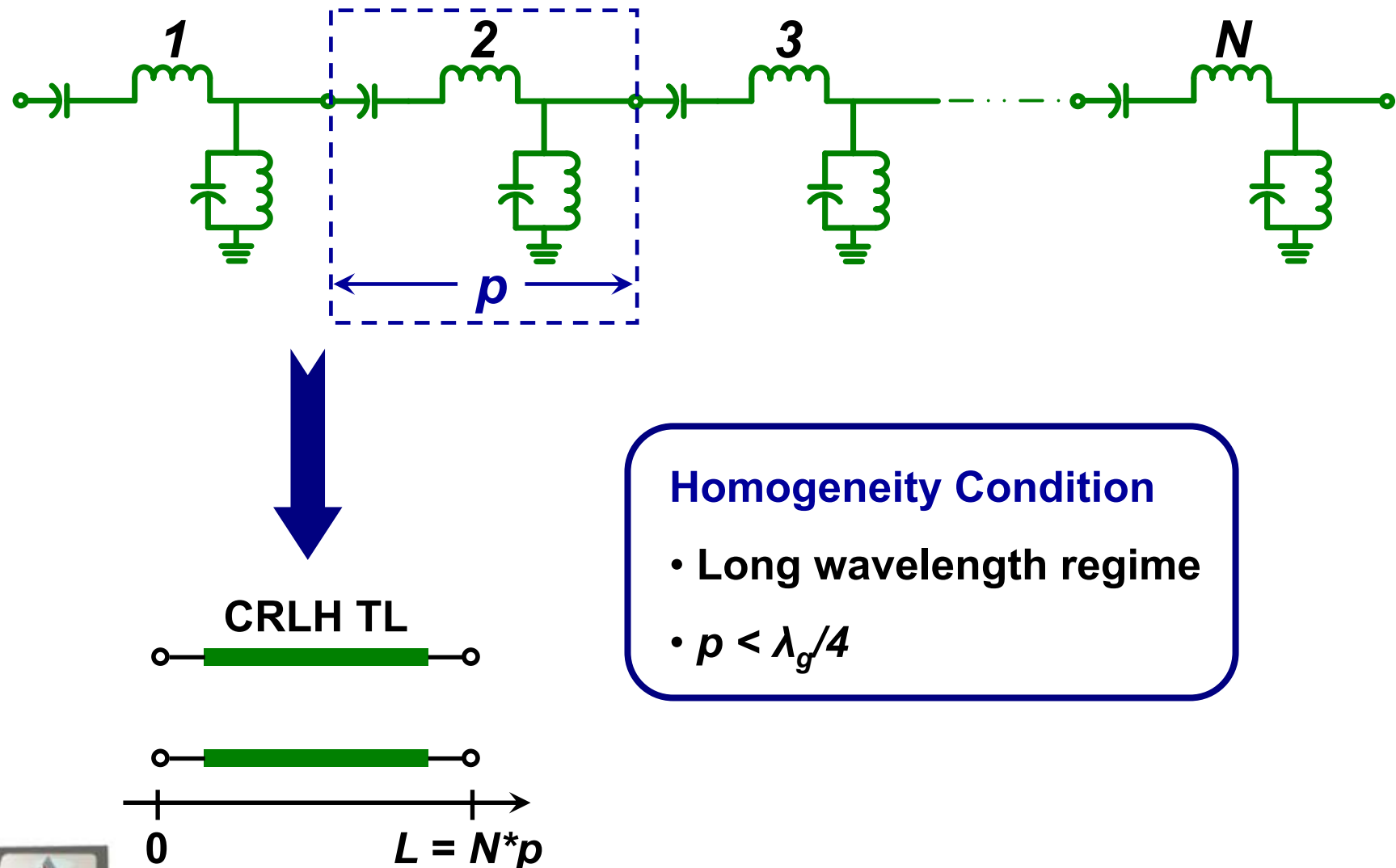
where

$$\omega_{se} = \frac{1}{\sqrt{C_L L_R}} \text{ and } \omega_{sh} = \frac{1}{\sqrt{C_R L_L}}$$

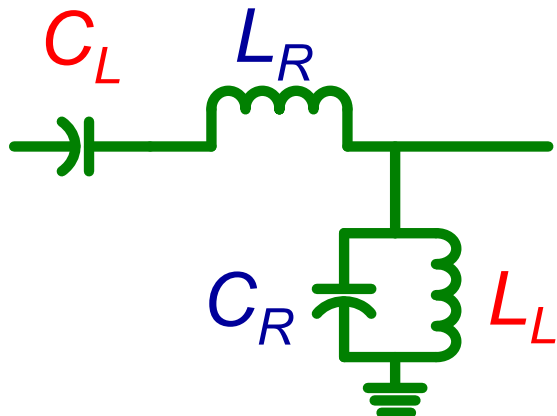


- Low frequencies: supports backward wave
- High frequencies: supports forward wave
- Two cases
  - ❖ Unbalanced:  $\omega_{se} \neq \omega_{sh}$
  - ❖ Balanced:  $\omega_{se} = \omega_{sh}$

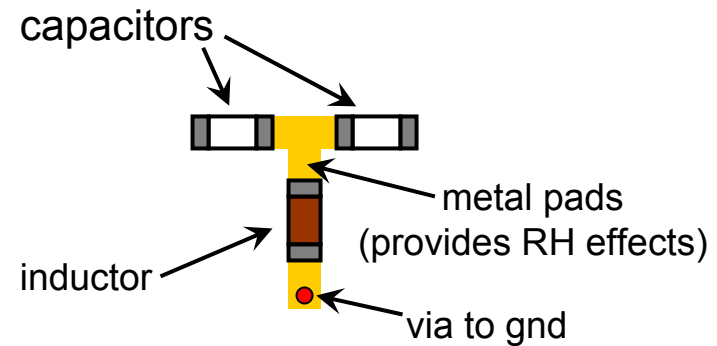
# CRLH Metamaterial



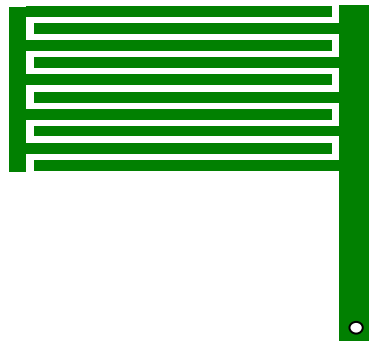
# CRLH Metamaterial – Physical Realization



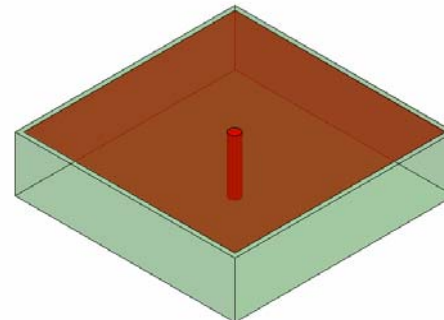
Composite right/left-handed (CRLH) unit-cell



Lumped element implementation



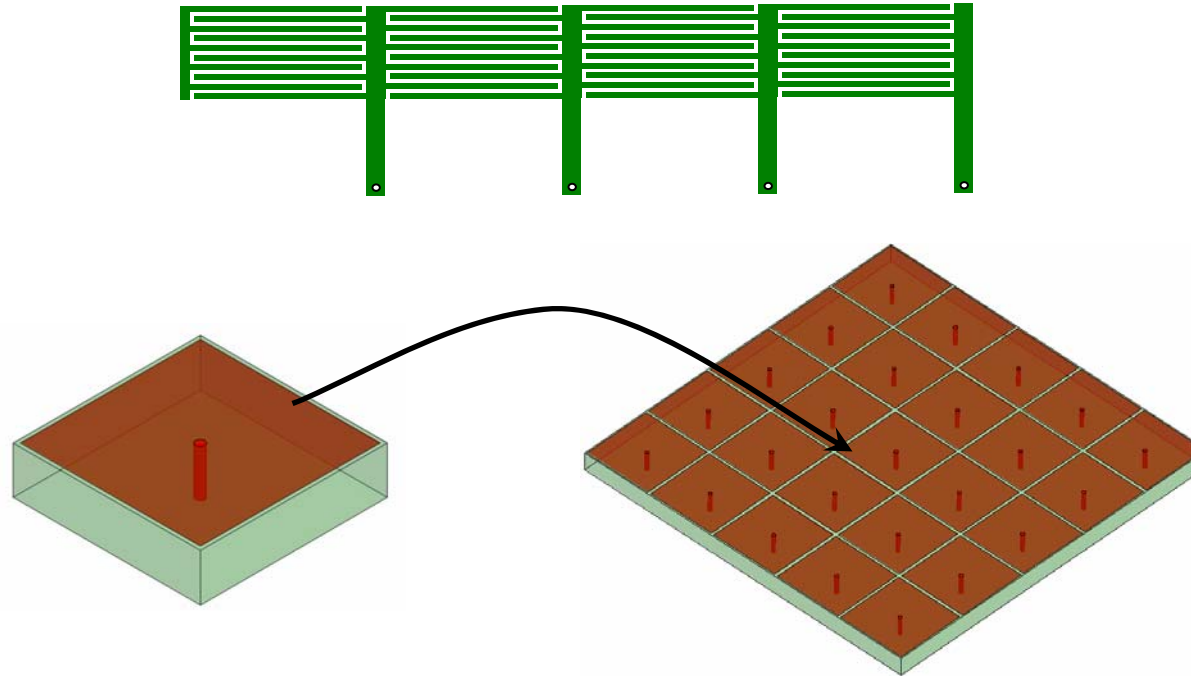
Distributed microstrip implementation based on interdigital capacitor



Distributed microstrip implementation based on Sievenpiper mushroom structure [5]

# CRLH – Implementation and Analysis

Cascade periodic unit-cell to form one- or two-dimensional CRLH metamaterial TL.



**How to Characterize a CRLH Unit-Cell**

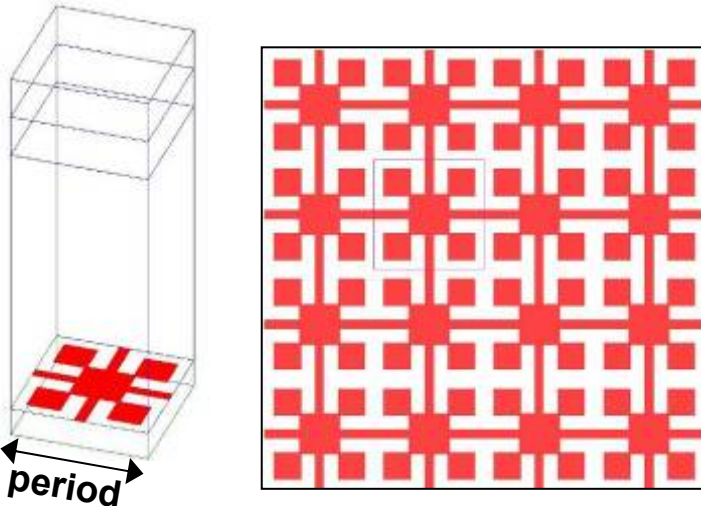
**Propagation Constant – Dispersion Diagram**

**Impedance – Bloch Diagram**



# Comparison of LHMs to PBGs and Filters

## Photonic Bandgap (PBG)



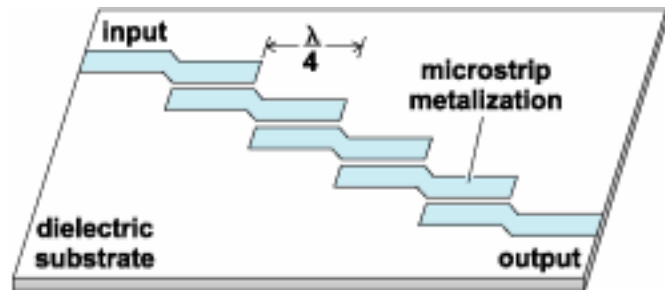
### Similarities

- periodic structures
- can be more than one-dimensional

### Differences

- PBGs have to be periodic; lattice period determines scattering
- PBG operated at frequencies where lattice period is multiple of  $\lambda_g/2$ ; LHMs operated at frequencies where period  $< \lambda_g/4$ .

## Filters



### Similarities

- periodic structures
- based on low-pass/high-pass structures

### Differences

- Filters generally designed to meet magnitude specifications; LHMs designed to meet both magnitude and phase.
- Node-to-node phase shifts of 180° required for filters.
- LHMs can be one-, two-, or three-dimensional and are used as bulk “mediums.”



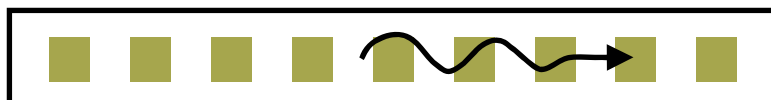
# Dominant-Mode Leaky Wave Antenna



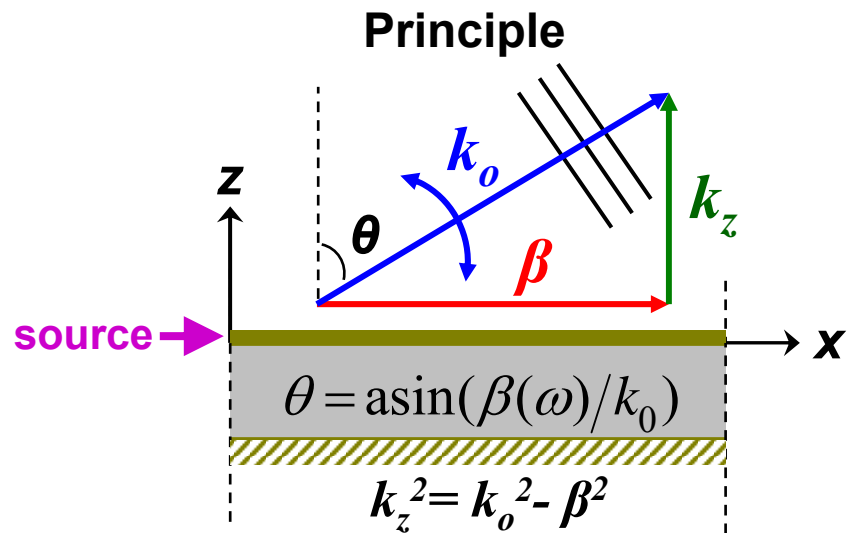
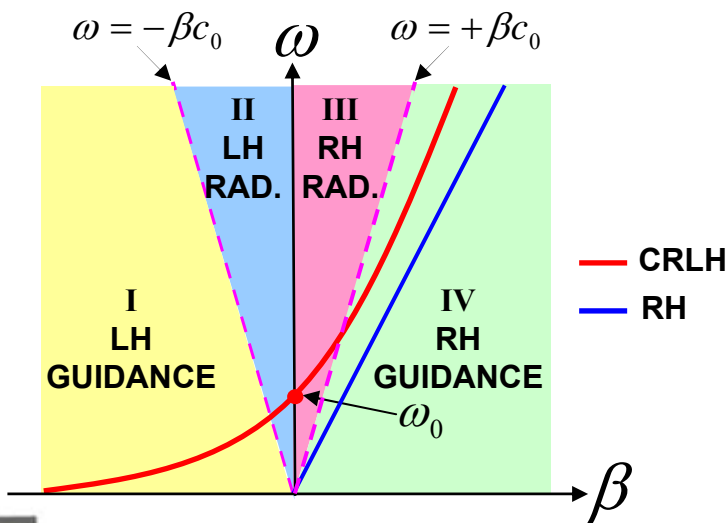
# Leaky-Wave Antenna Theory



Conventional RH Leaky-Wave Antenna  
(operated at higher-order mode)



CRLH Leaky-Wave Antenna [6]  
(operated at dominant mode)



## Characteristics:

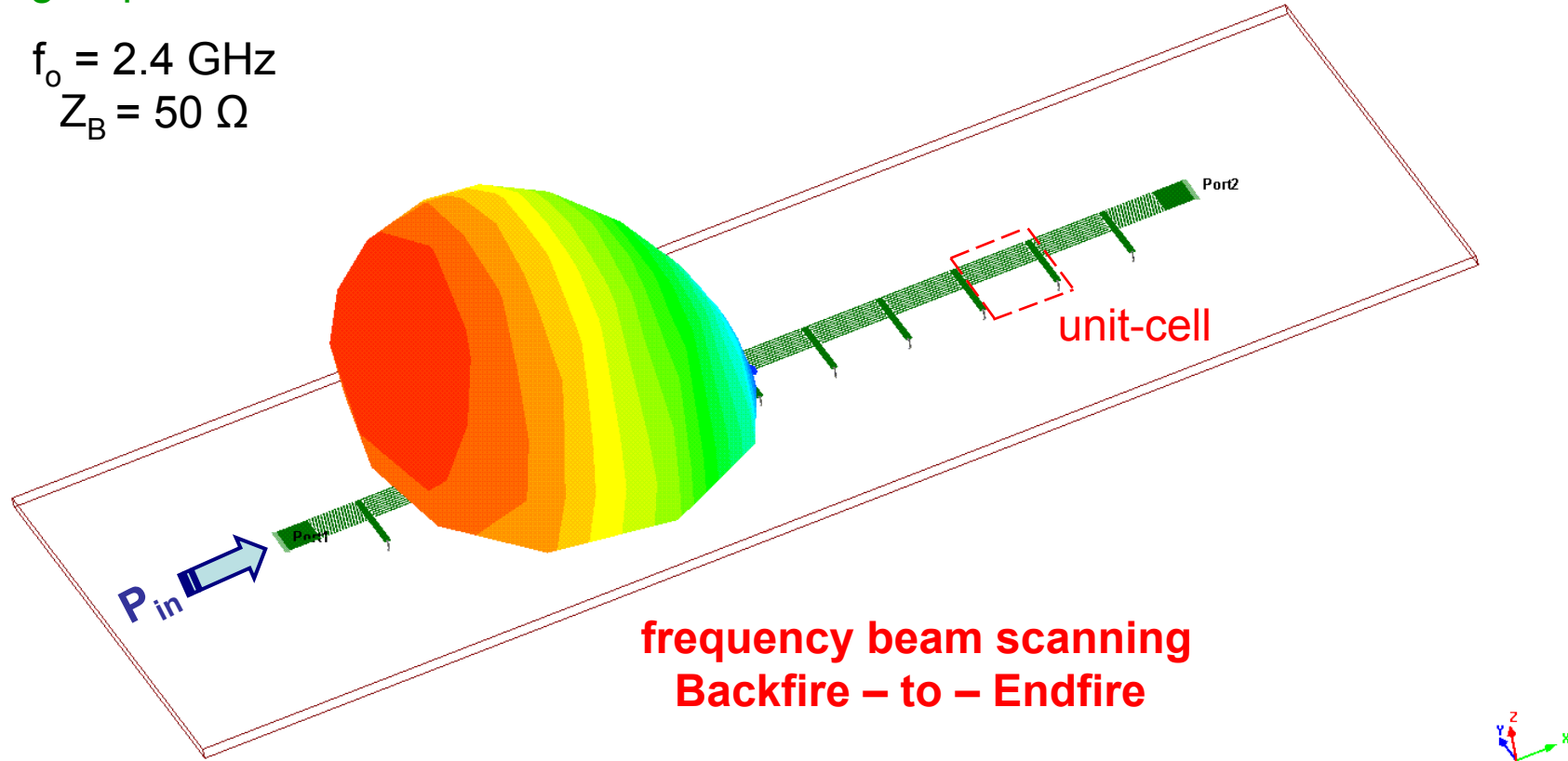
- Operating in leaky regions
- **II : BACKWARD (  $\beta < 0$  )**
- **III : FORWARD (  $\beta > 0$  )**
- **BROADSIDE radiation (  $\beta = 0$  )**  
*balanced case:  $v_g(\beta = 0) \neq 0$*
- **Fundamental mode**

# 1-D Dominant Mode Leaky-Wave Antenna

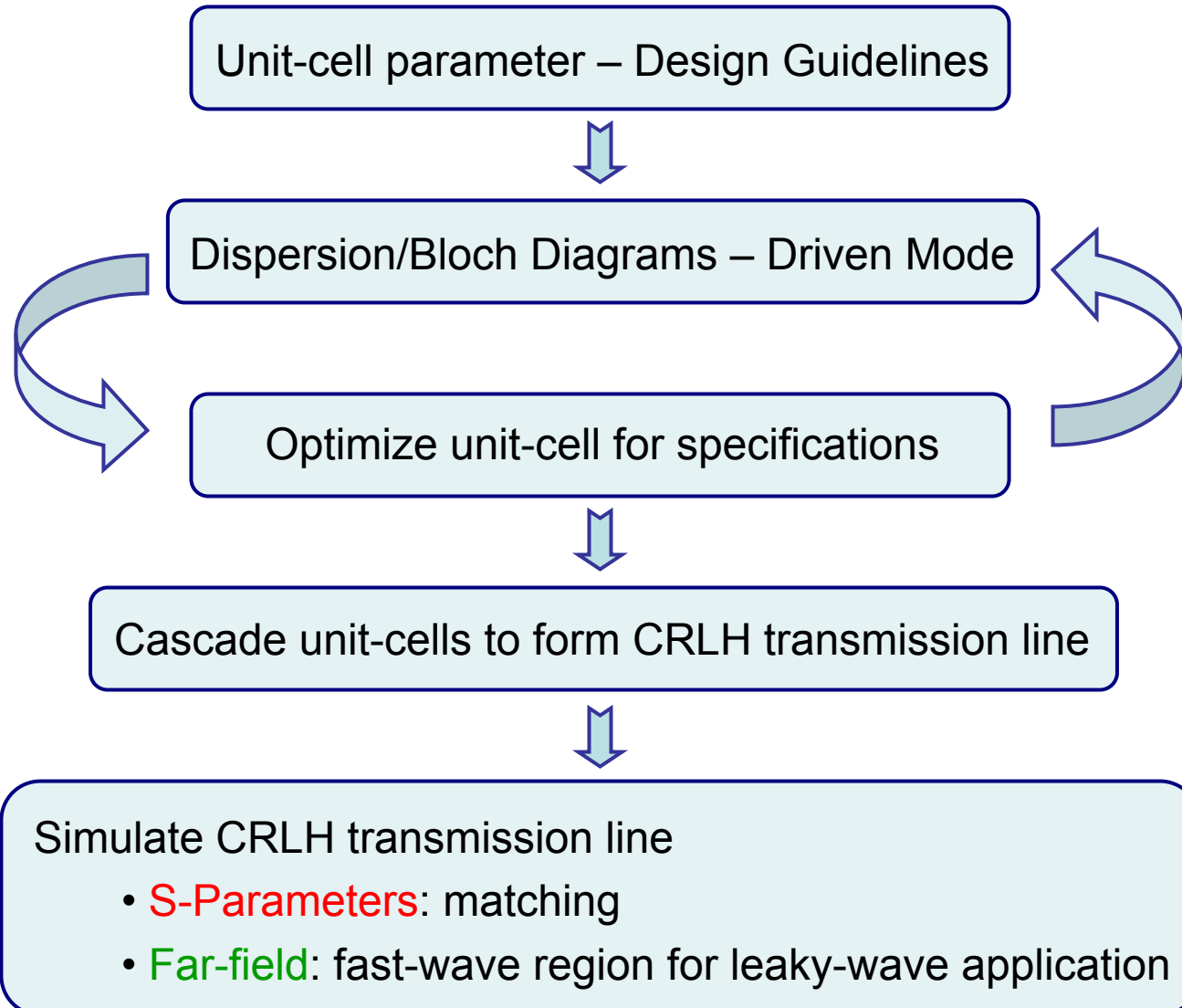
## 3-D Far-field Pattern for Several Frequencies

### Design Specifications

$$f_o = 2.4 \text{ GHz}$$
$$Z_B = 50 \Omega$$



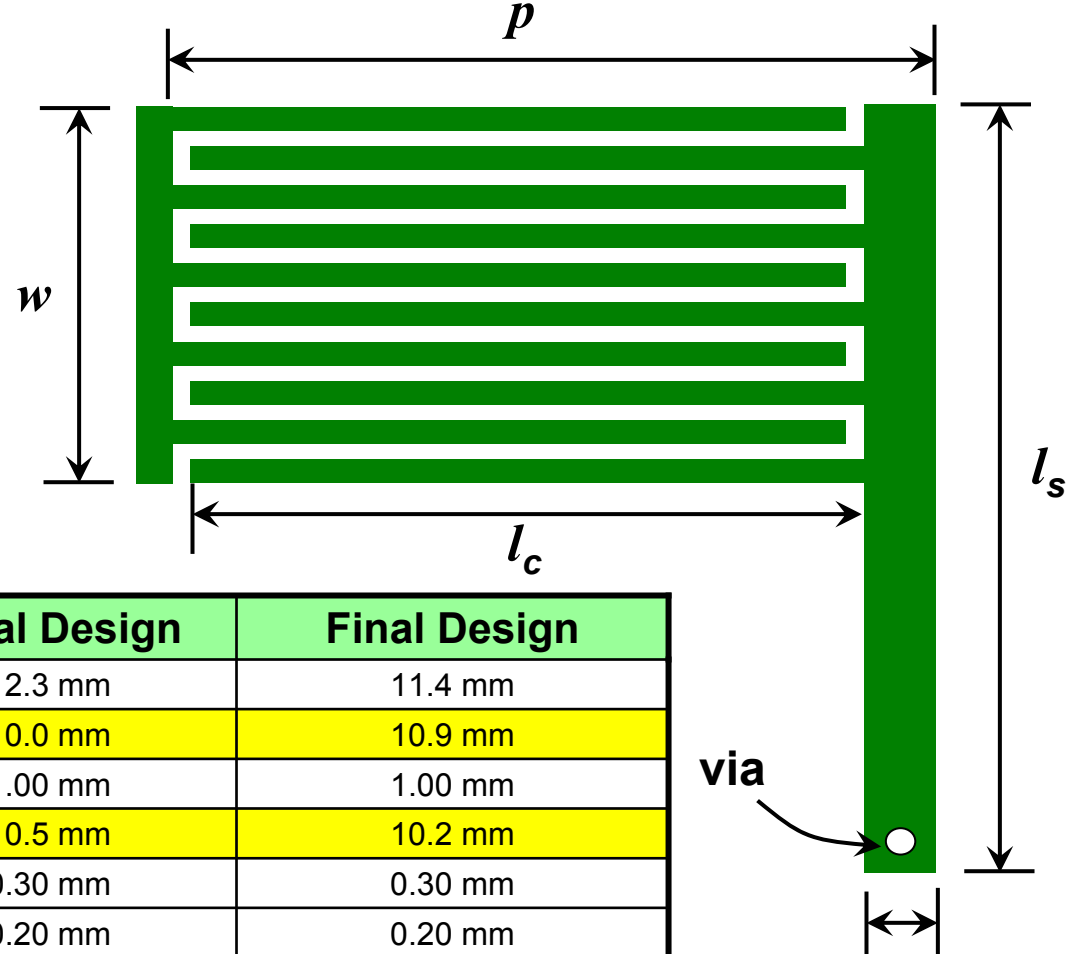
# Design Flow



# 1-D CRLH Unit-Cell (Interdigital)

- Distributed unit-cell

- series capacitance provided by interdigital capacitor
- shunt inductance provided from shorted stub
- shunt capacitance from top metal to ground plane
- series inductance from current on interdigital capacitor



Variables	Initial Design	Final Design
unit-cell period	$p$	12.3 mm
stub length	$l_s$	10.0 mm
stub width	$w_s$	1.00 mm
interdigital finger length	$l_c$	10.5 mm
interdigital finger width	$w_c$	0.30 mm
spacing between fingers	$S$	0.20 mm
via radius	$r$	0.12 mm
substrate height	$h$	1.57 mm
substrate permittivity	$\epsilon_r$	2.2



# 1-D CRLH Unit-Cell Design Guidelines\*

For 2-D space scanning, we need to design a balanced ( $\omega_{se} = \omega_{sh}$ ) CRLH unit-cell so that there is a seamless transition from LH to RH operation.

1. Choose center frequency,  $f_o$ , which represents broadside radiation. ( $f_o=2.4$  GHz)
2. Calculate width required to obtain  $Z_o$ , set  $w$  to this value. ( $w\sim 5.0$  mm)
3. Set stub width,  $w_s$ , to 20% of  $w$ . ( $w_s=1.0$  mm)
4. Set stub length ( $l_s^i = l_s - w$ ) to  $w$ ; the electrical length of the stub has to be less than  $\pi/2$ .

5. Set the number of fingers,  $N$ , to 8 or 10. Then determine required  $w_c$  and  $S=2w_c/3$ .  $N=10$  chosen.

$$w_c \approx \frac{w}{\left(\frac{5N}{3} - \frac{2}{3}\right)} \approx 0.3 \text{ mm}$$

$$S = 0.2 \text{ mm}$$

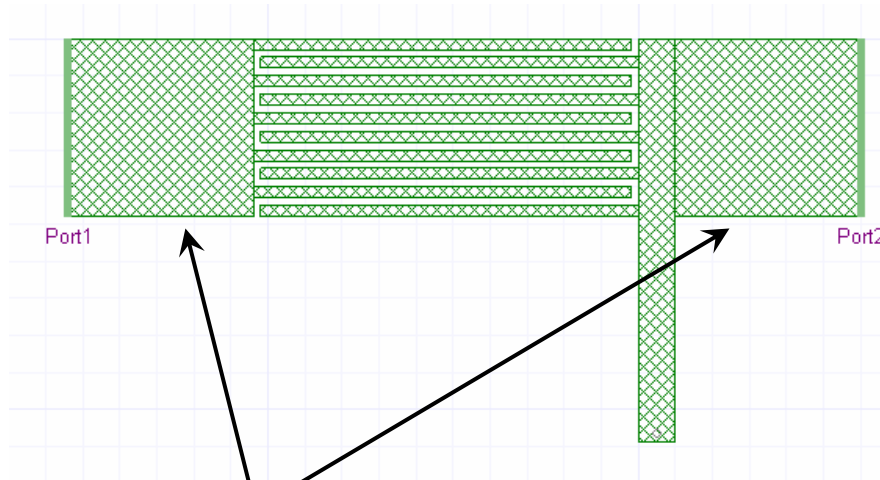
6. Calculate length of interdigital finger.

$$l_c \approx \frac{\lambda_g}{8} \approx \frac{c_o}{8f_o \sqrt{\epsilon_r}} \approx 10.5 \text{ mm}$$

\* Guidelines have been test on Rogers Duroid 5870 ( $\epsilon_r=2.33$ ) and 5880 ( $\epsilon_r=2.2$ ) for various substrate heights; for high permittivity substrate, the number of fingers should be reduced.



# Dispersion/Bloch Diagram Extraction



Design Specifications

$$f_o = 2.4 \text{ GHz}$$

$$Z_B = 50 \Omega$$

extra section of microstrip (5 mm each)

Planar EM simulation

S-Parameter extraction

$$\beta p = \cos^{-1} \left( \frac{1 - S_{11}S_{22} + S_{12}S_{21}}{2S_{21}} \right)$$

$$Z_B = \frac{2jZ_o S_{21} \sin(\beta p)}{(1 - S_{11})(1 - S_{22}) - S_{21}S_{12}}$$

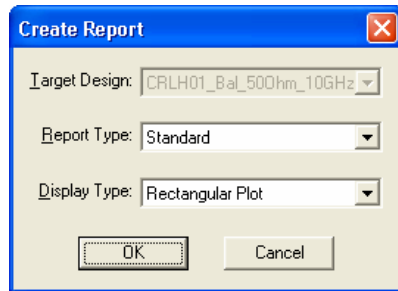


# Dispersion Diagram Extraction

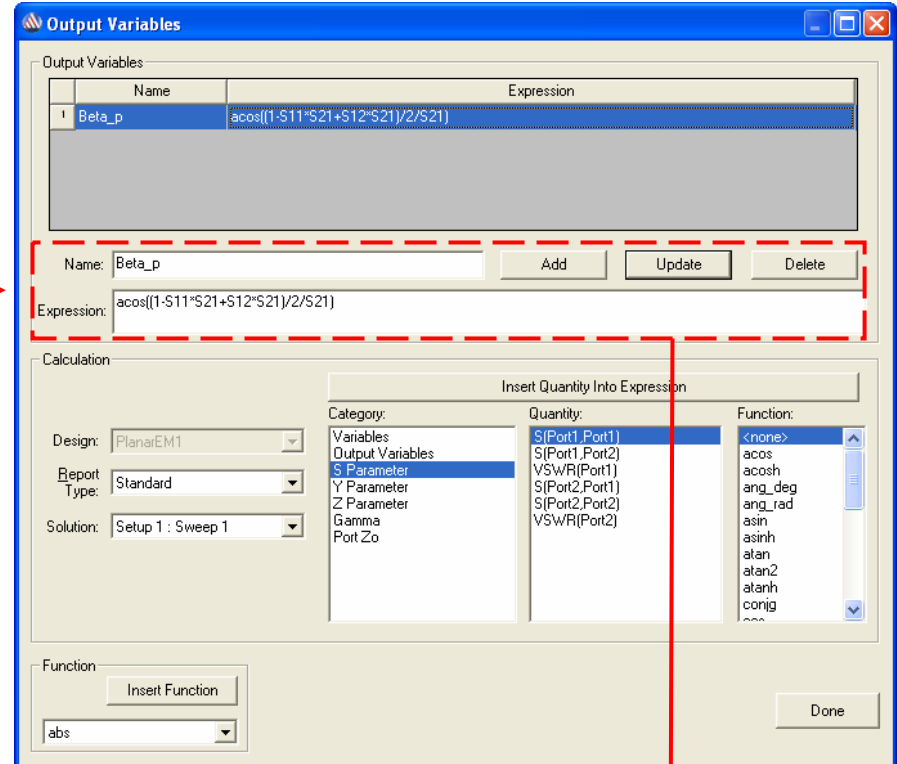
Setup dispersion equation; this can be obtained directly from the S-parameters.

$$\beta p = \cos^{-1} \left( \frac{1 - S_{11}S_{22} + S_{12}S_{21}}{2S_{21}} \right)$$

Go to *Results > Create Report*

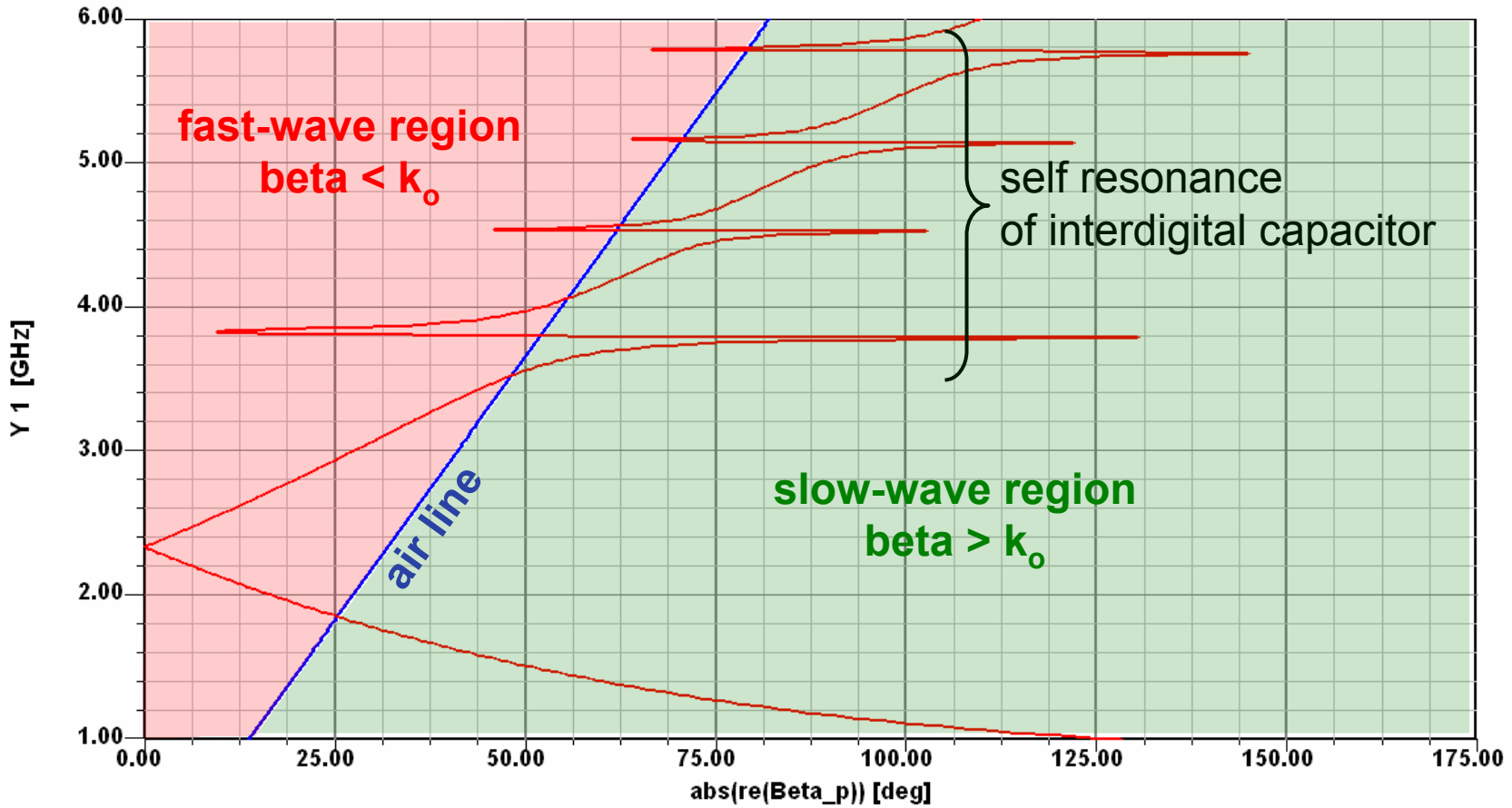


Then click on *Output Variables*



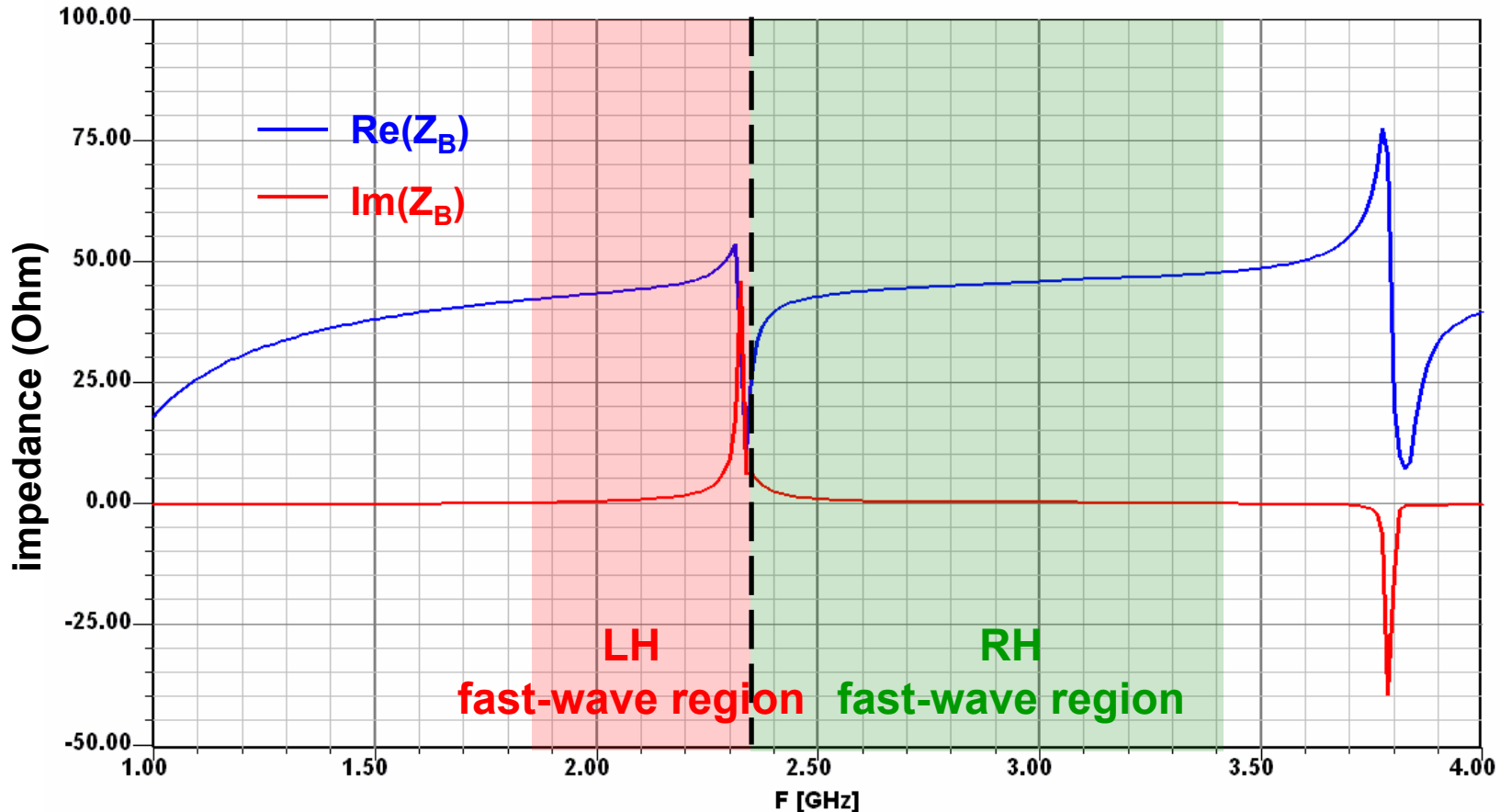
# Dispersion Diagram

Final Design Dispersion Diagram in Ansoft Designer

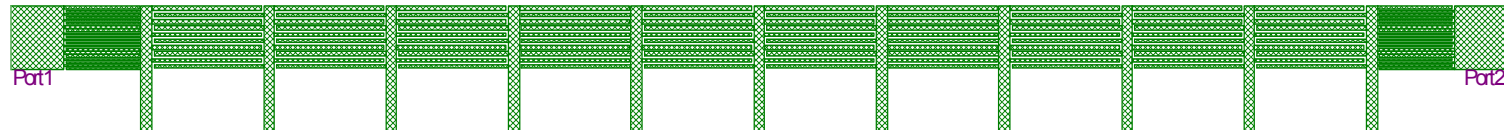


# Bloch Impedance Diagram

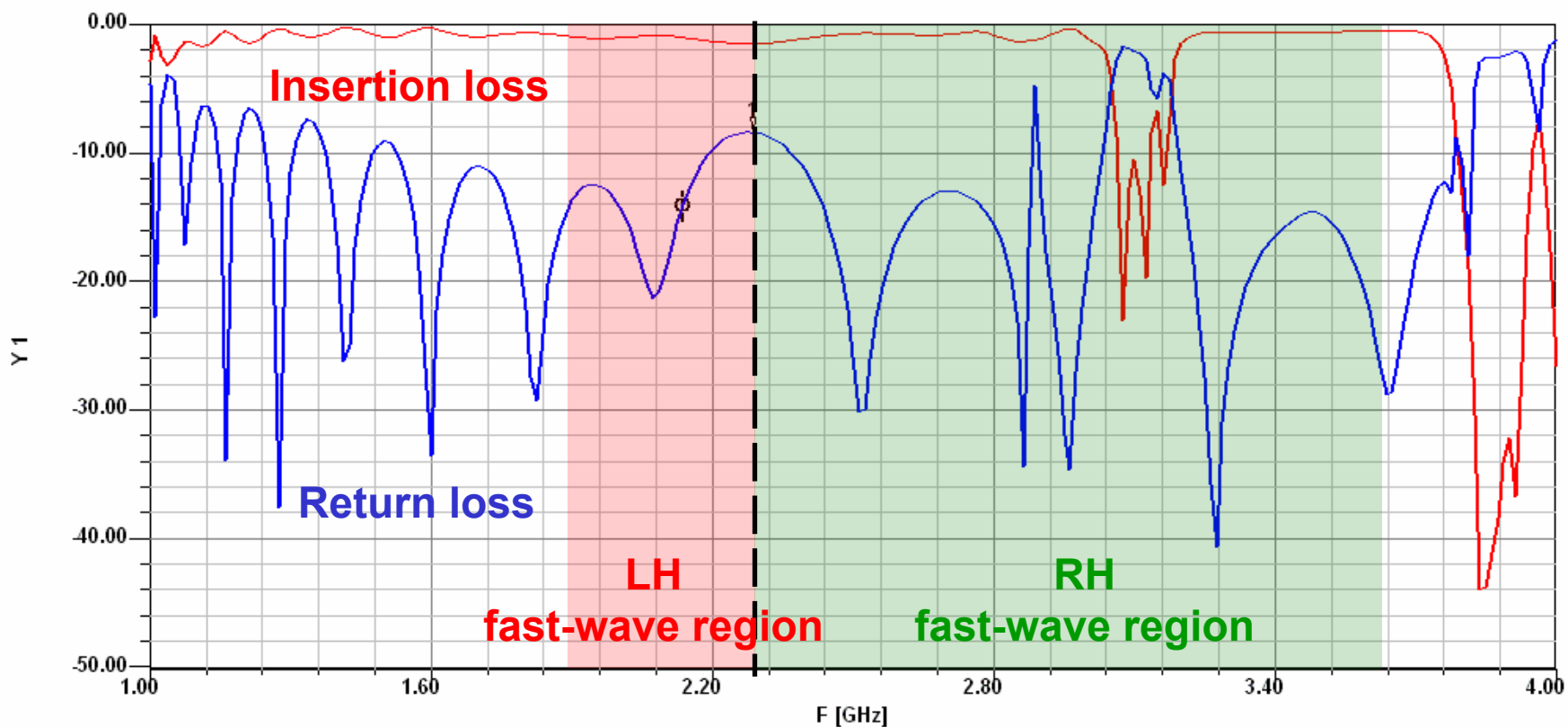
## Resulting Bloch Impedance Diagram in Ansoft Designer



# 10-Cell CRLH Leaky-Wave Antenna

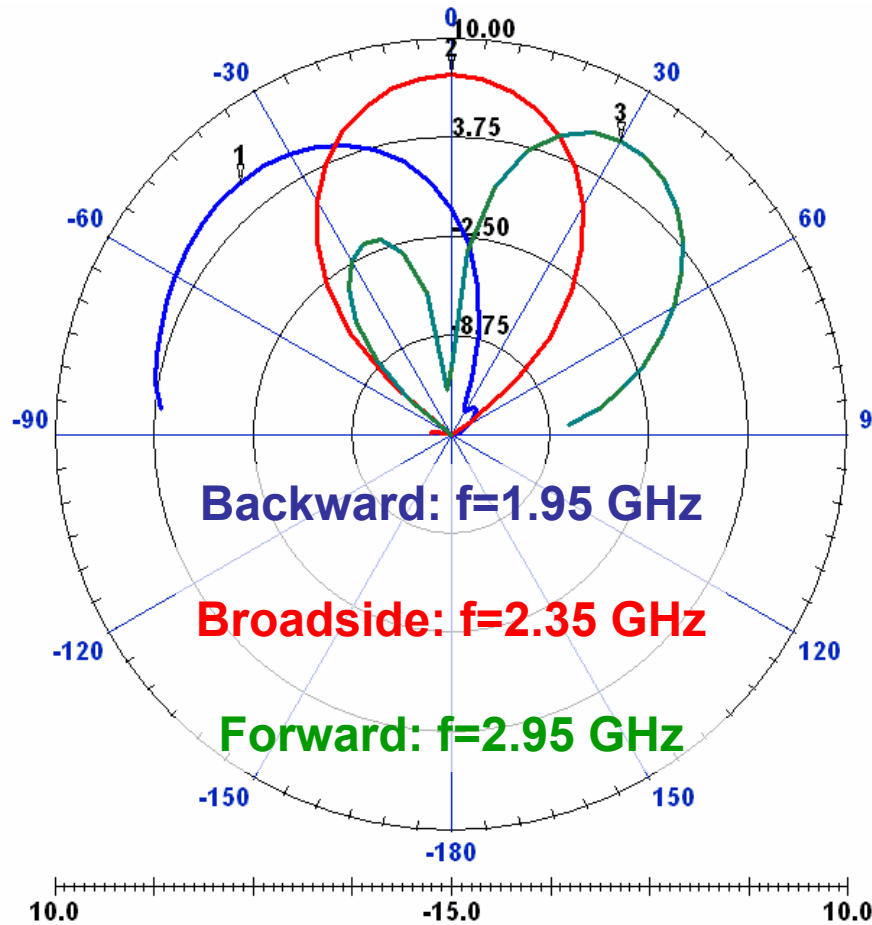


Return/Insertion Loss



# 10-Cell CRLH Leaky-Wave Antenna

## Far-field Pattern for Several Frequencies

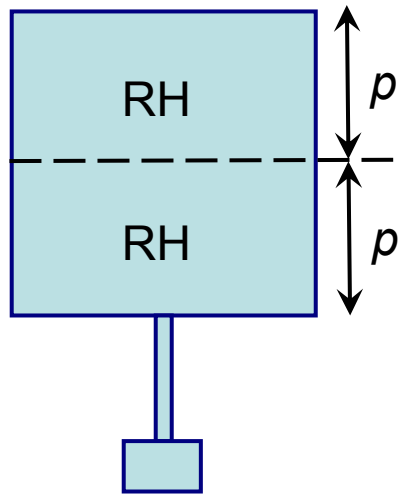


# Small Metamaterial Antennas



# Resonant Antenna Theory

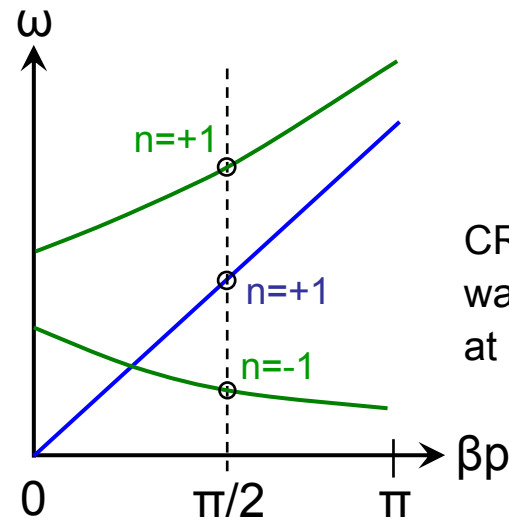
Conventional RH Patch Antenna  
(treat as periodic, consisting of 2 RH “unit-cells”)



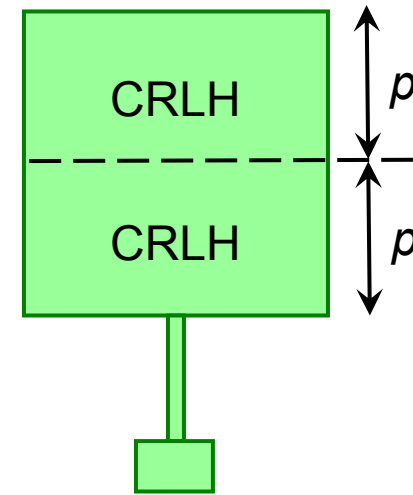
$n = +1, +2, \dots$

resonance condition

$$\beta_n = \frac{n\pi}{2p}$$



CRLH Patch Antenna  
(2 CRLH unit-cells)

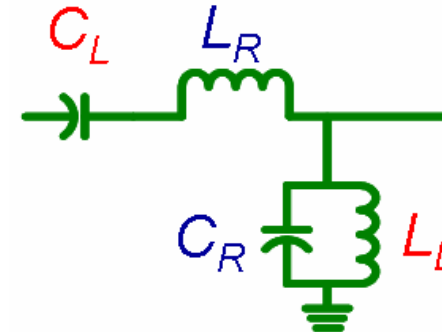
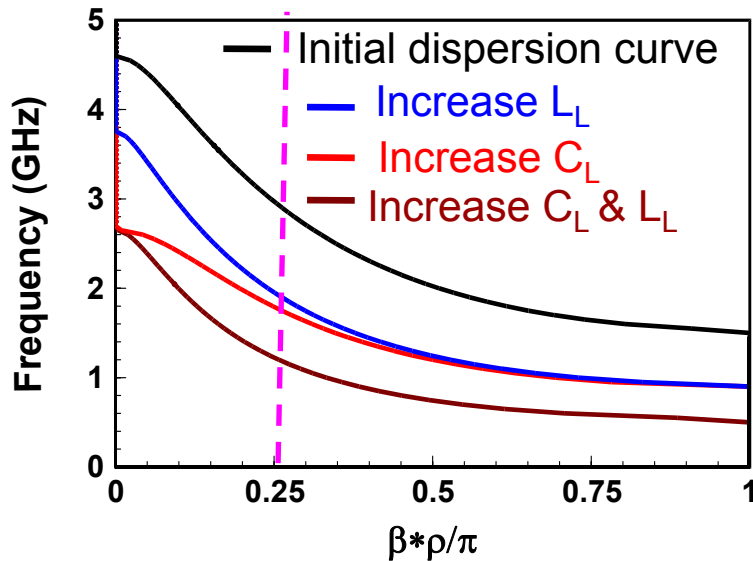


$n = 0, \pm 1, \pm 2, \dots$

CRLH can have same half-wavelength field distribution, but at much lower frequency

# 1.0 GHz CRLH n=-1 Antenna [7]

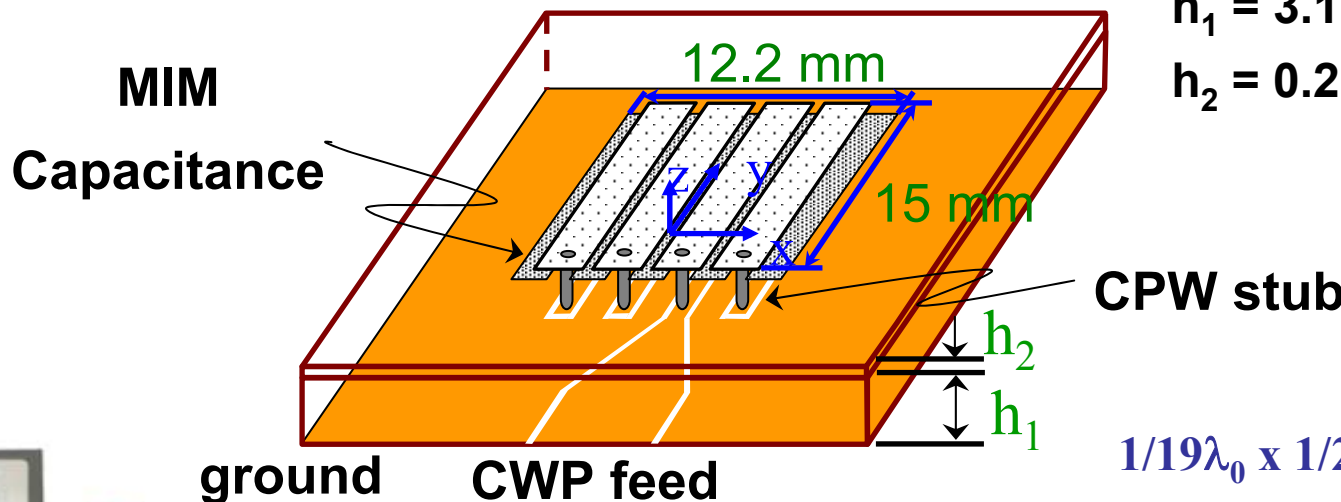
for 4 unit-cells



$n = -1$  mode is used

$h_1 = 3.16$  mm

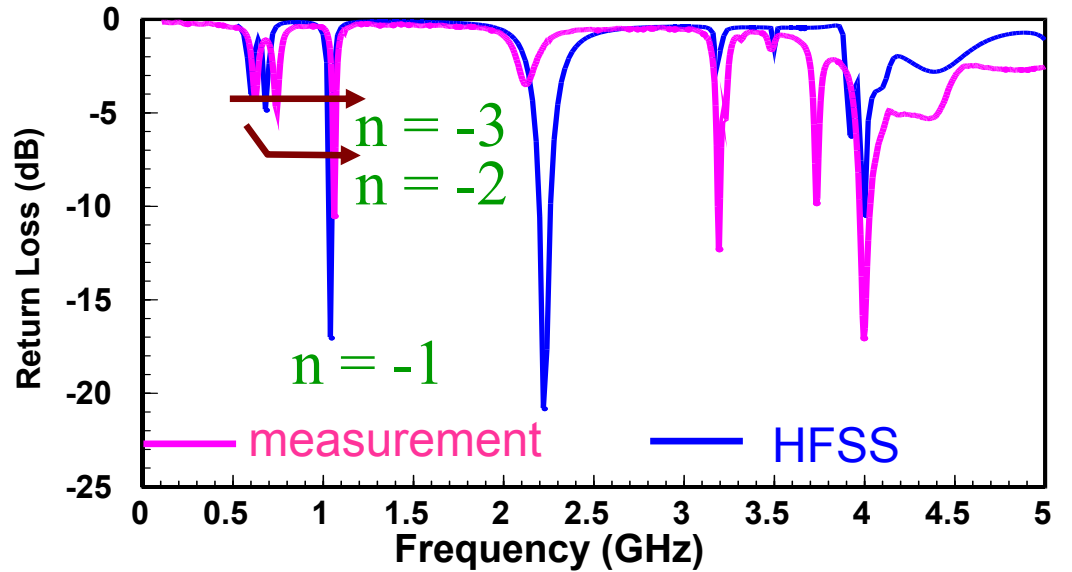
$h_2 = 0.254$  mm



$1/19\lambda_0 \times 1/23\lambda_0 \times 1/88\lambda_0$

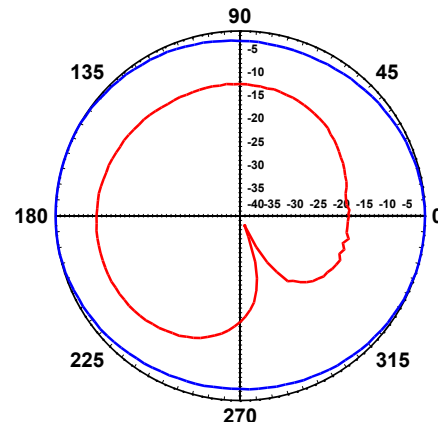
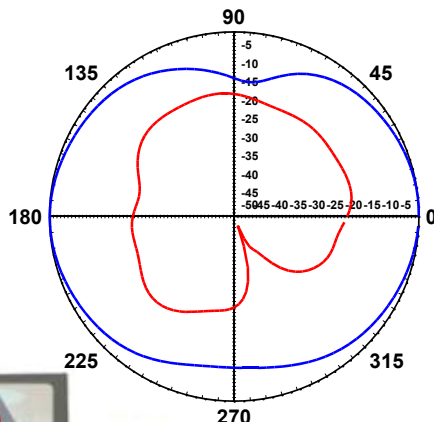


# 1.0 GHz CRLH n=-1 Antenna [7]

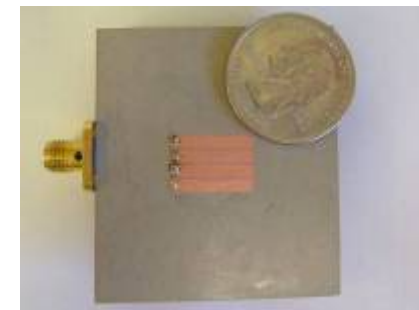


— E-copol (x-z plane)  
— E-xpol (x-z plane)

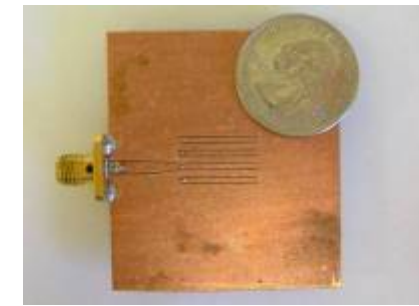
— H-copol (y-z plane)  
— H-xpol (y-z plane)



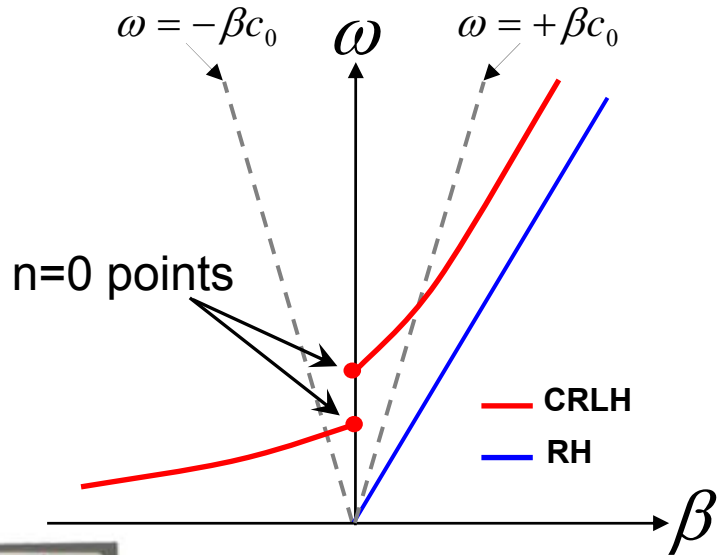
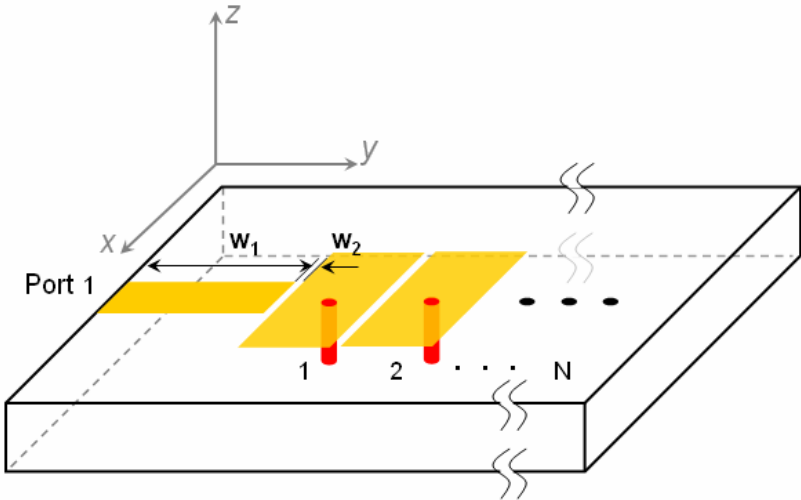
top view



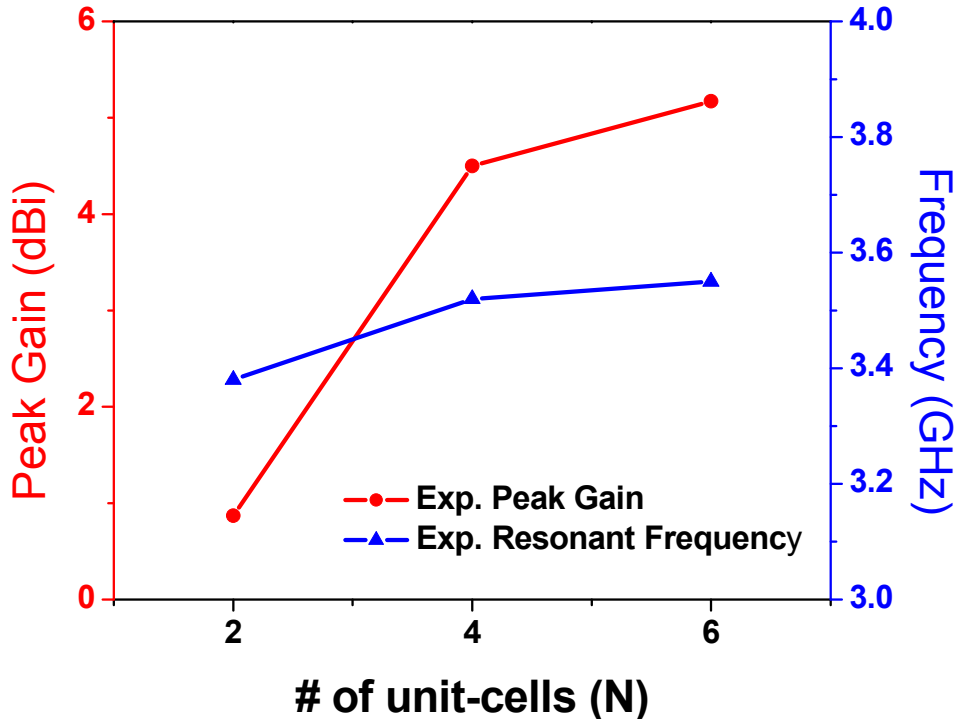
back view



# CRLH n=0 Antenna (Monopolar) [8]



## Experimental Results

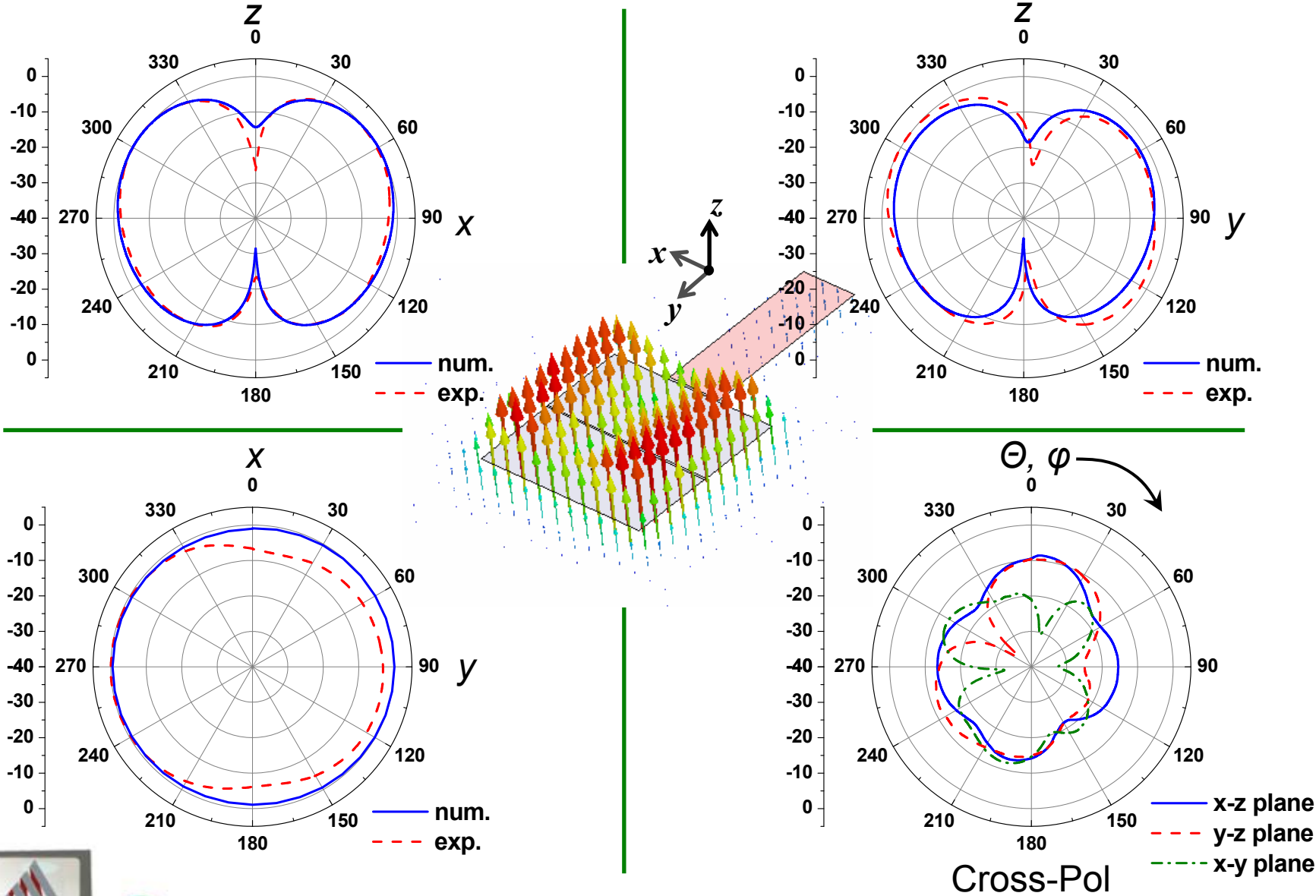


As  $N$  increases...

- Gain increases.
- Resonant frequency does not change much.



# CRLH n=0 Antenna (Monopolar)

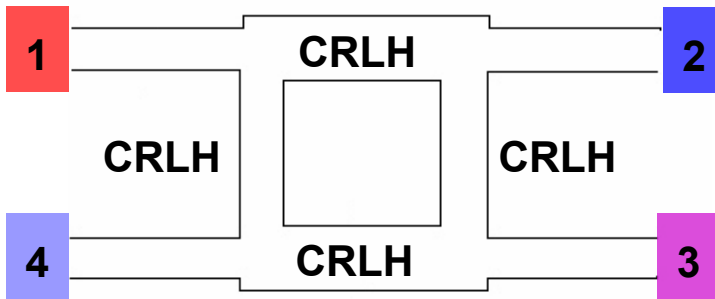


# Dual-/Multi-Band Metamaterial Components



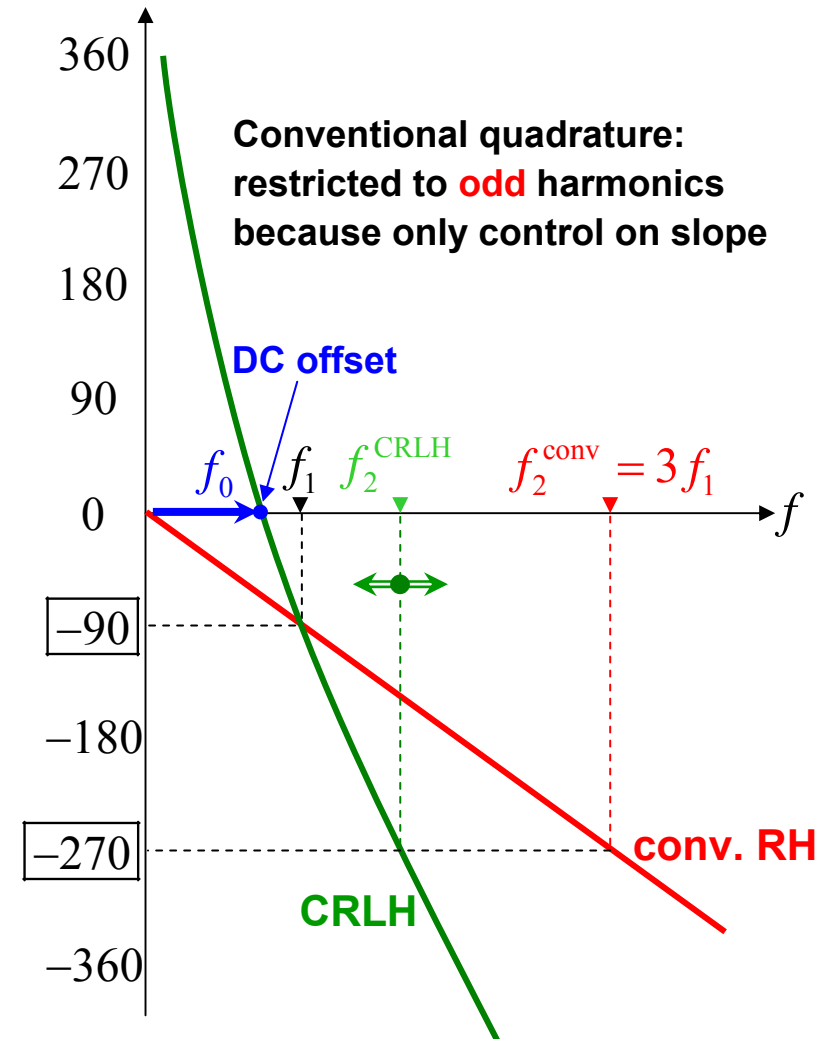
# Dual-Band Hybrid Coupler

## CRLH / CRLH hybrid [9]

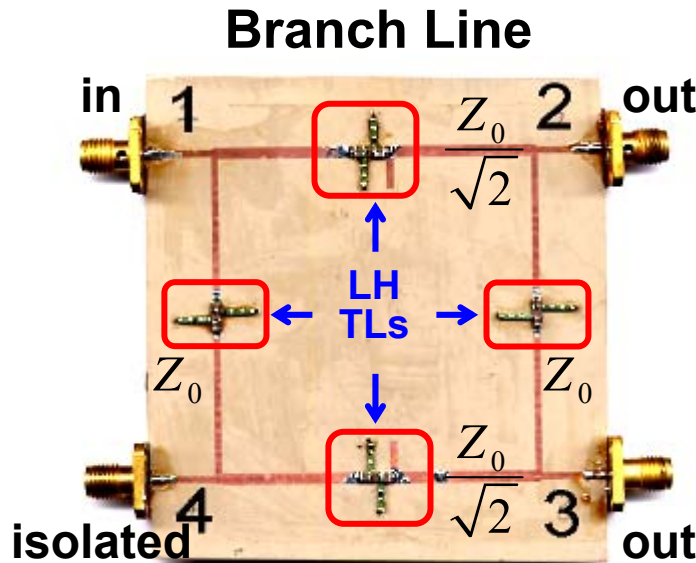


### Characteristics:

- **dual-band functionality for an arbitrary pair of frequencies  $f_1, f_2$**
- **principle:** transition frequency ( $f_0$ ) provides **DC offset** additional degree of freedom with respect to the **phase slope**
- **applications in multi-band systems**

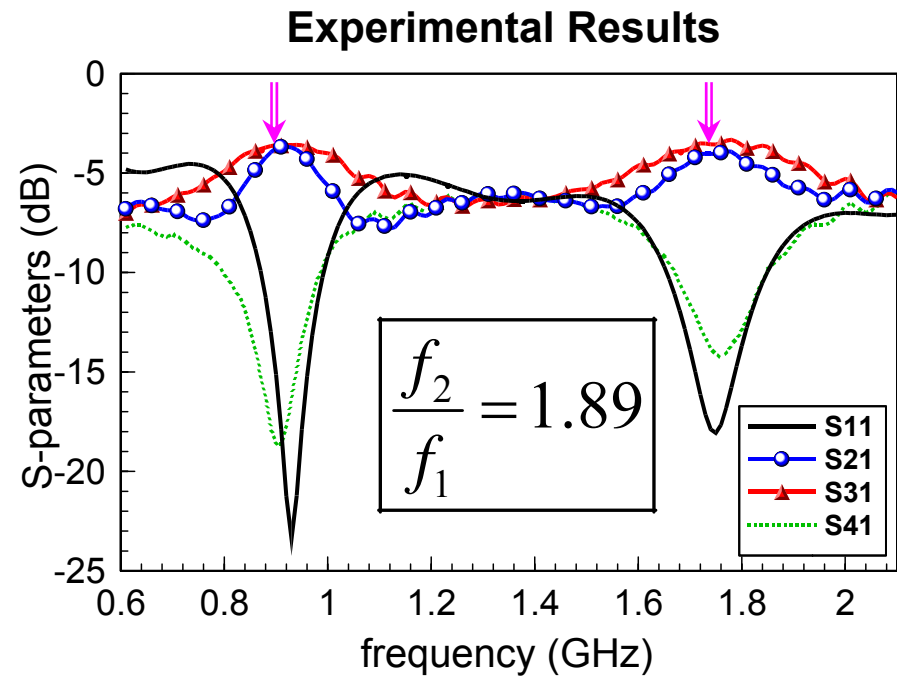


# Dual-Band Hybrid Coupler



Band # 1: 0.92 GHz

Band # 2: 1.74 GHz

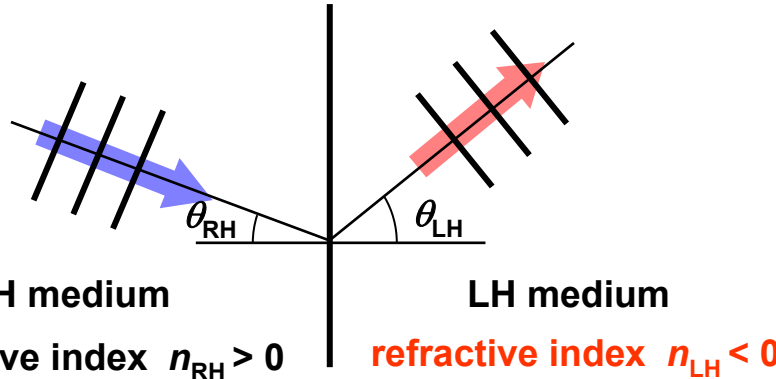


# Negative Refractive Index Lenses

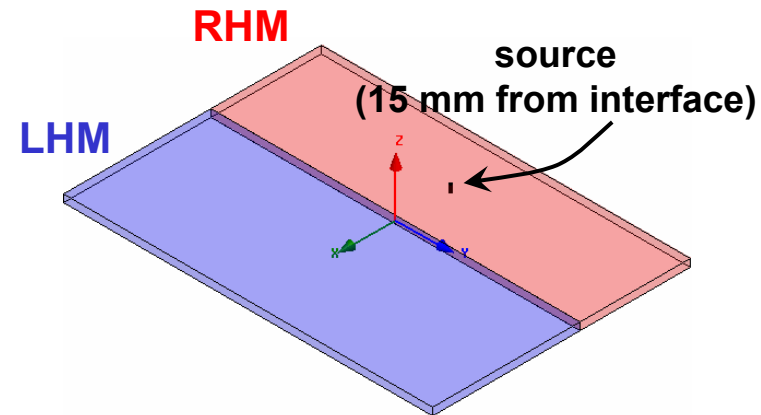


# Negative Refractive Index Flat Lens [10]

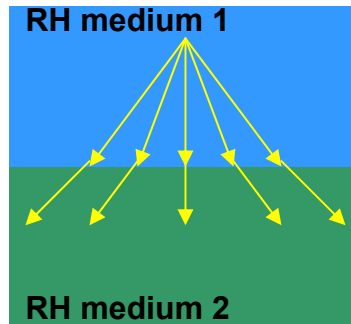
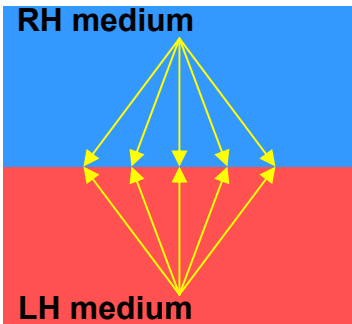
$$(n_{\text{LH}}) \sin \theta_{\text{LH}} = (n_{\text{RH}}) \sin \theta_{\text{RH}}$$



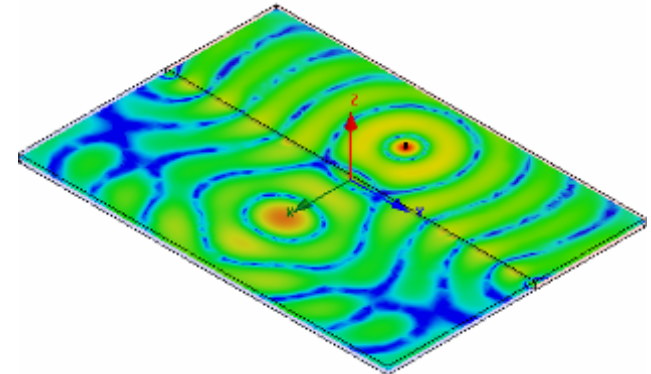
Effective medium HFSS simulation



Possibility of realizing a flat lens

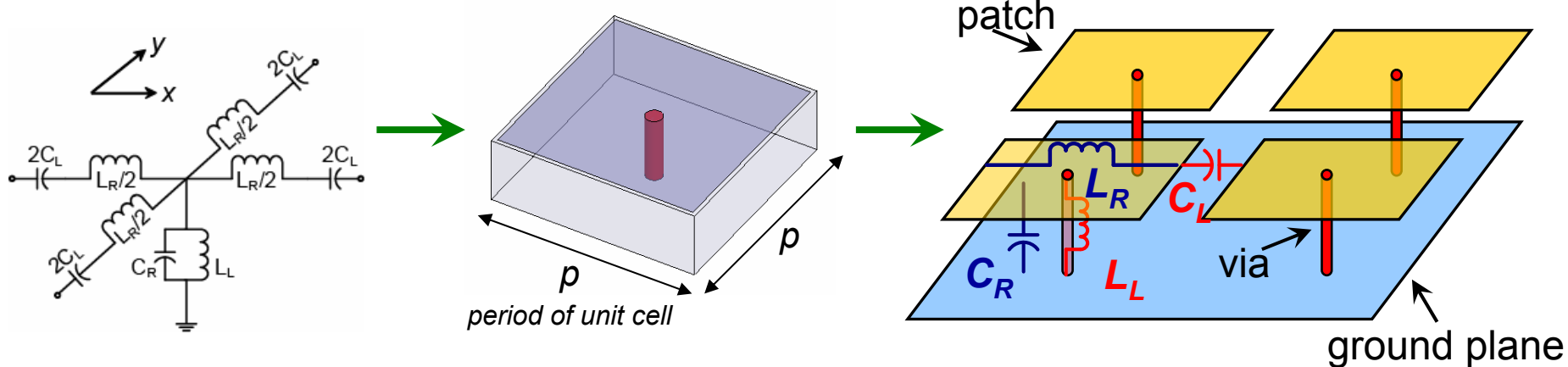


E-field magnitude



# Two-Dimensional CRLH Realization

Based on Sievenpiper High-Impedance Structure

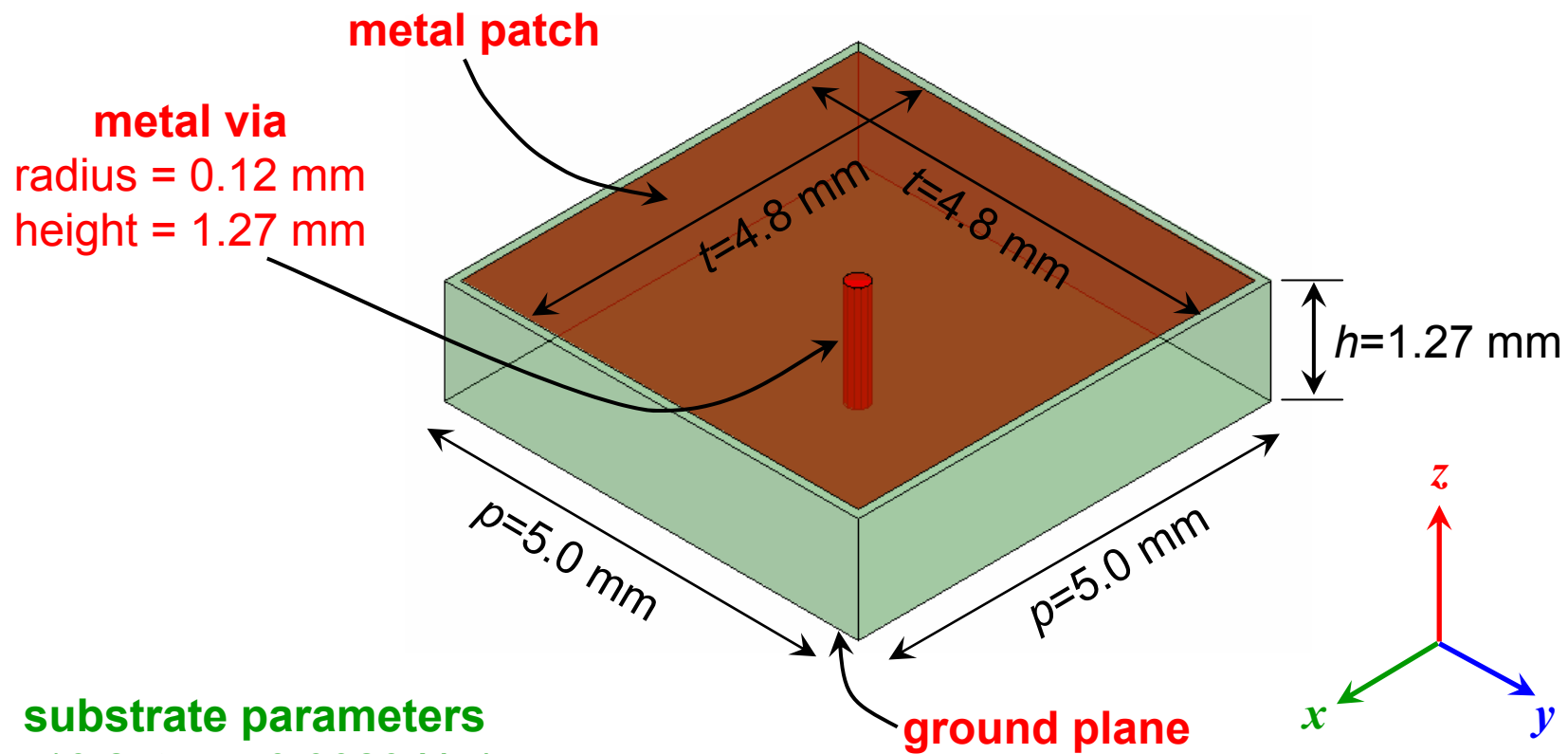


How to obtain dispersion characteristics?

1. Drivenmode Approach – Simple, quick, 1-D dispersion diagram.
2. Eigenmode Approach – Requires more processing time, accounts for mode coupling, 2-D dispersion diagram.



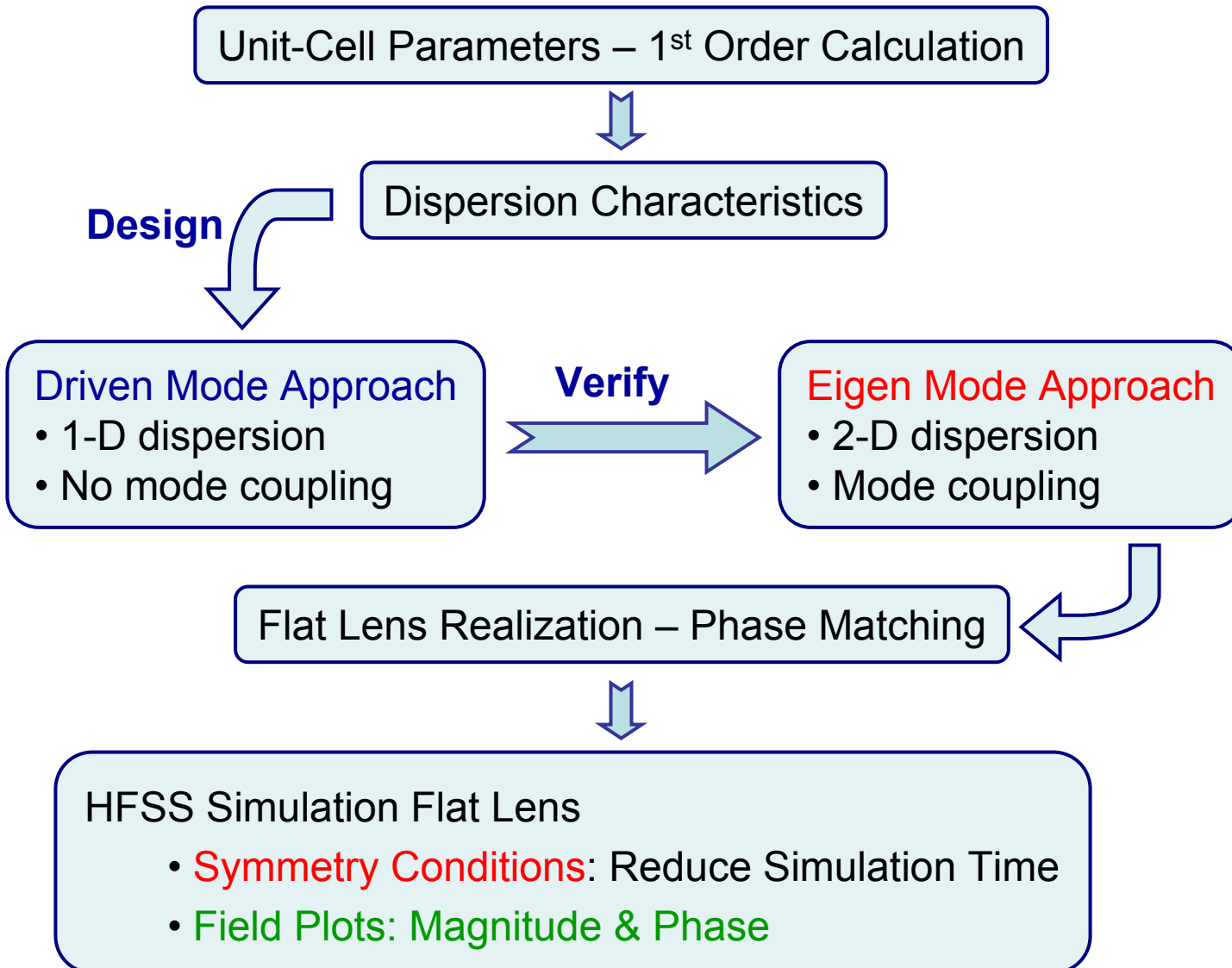
# Unit-Cell Setup: Physical Details



\* patch, via, and ground plane are assigned as copper.

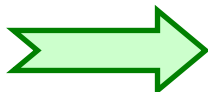
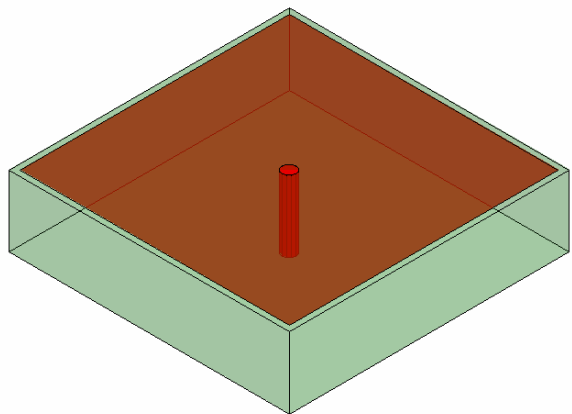


# Design Flow

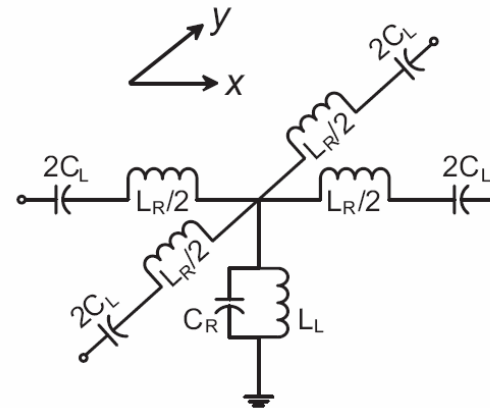


# Sievenpiper Unit-Cell: 1<sup>st</sup> Order Calculation

distributed unit-cell



equivalent circuit model



$$f_{sh} = 1/\{2\pi\sqrt{C_R \times L_L}\}$$

series capacitance:  $C_R \sim \text{substrate permittivity} \times (\text{patch area}/\text{substrate height})$

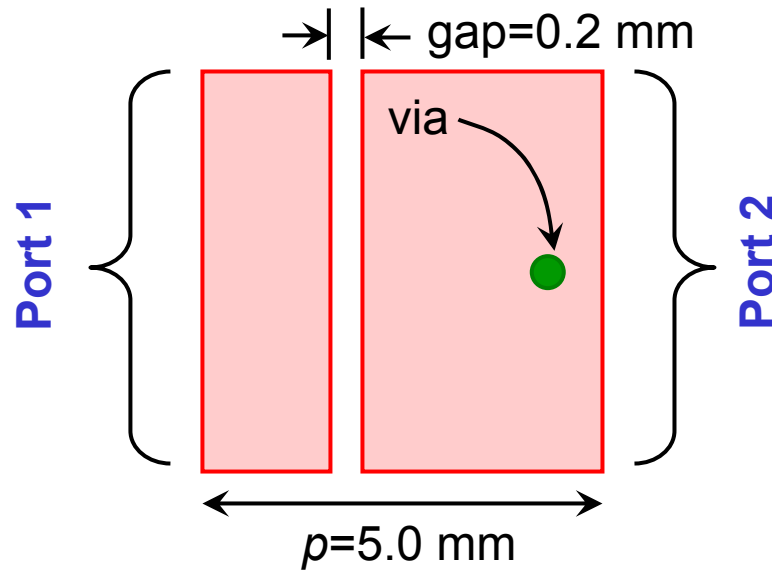
shunt inductance:  $L_L \sim 0.2 \times \text{substrate height} \times \ln[(2 \times \text{substrate height}/\text{via radius}) - 1]$

\* Left-handed mode will always occur below the shunt resonance ( $\omega_{sh}$ ). Therefore, design dimensions such that  $\omega_{sh}$  occurs at higher limit of frequency of interest.

$f_{sh} \sim 5 \text{ GHz}$  for the dimensions shown in previous slide.



# Sievenpiper Unit-Cell: Driven Mode



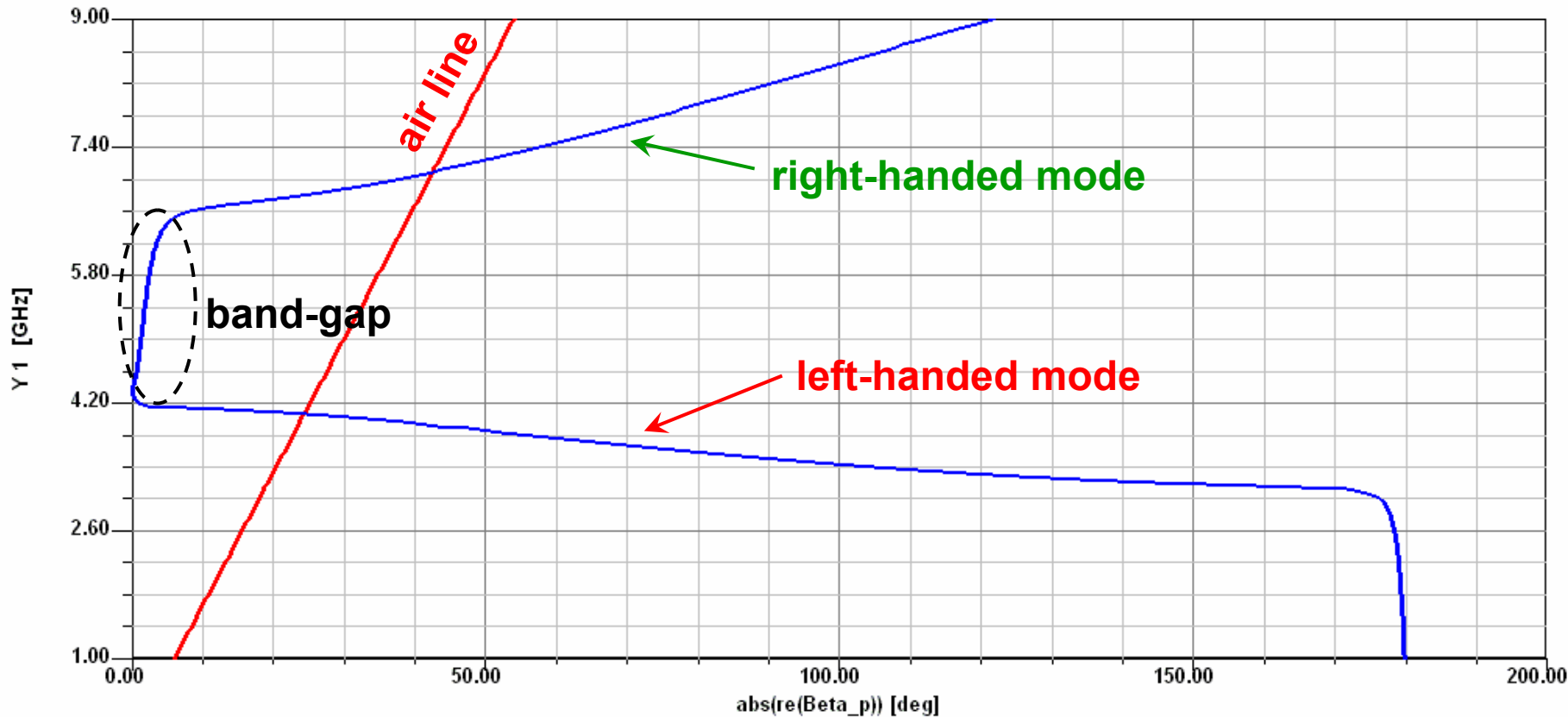
- Modify unit-cell so that ports can be placed on it, while keeping dimensions the same. Unit-cell becomes asymmetrical.
- Run driven mode solution; set mesh frequency to  $\omega_{sh}$  from 1<sup>st</sup> order calculation.
- Obtain S-parameters, use following expression to calculate propagation constant.

Name:	<input type="text" value="Beta_p"/>	<input type="button" value="Add"/>	<input type="button" value="Update"/>	<input type="button" value="Delete"/>
Expression:	<input type="text" value="acos([1-S11*S21+S12*S21]/2/S21)"/>			

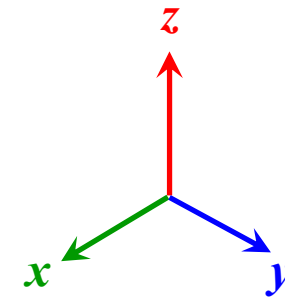
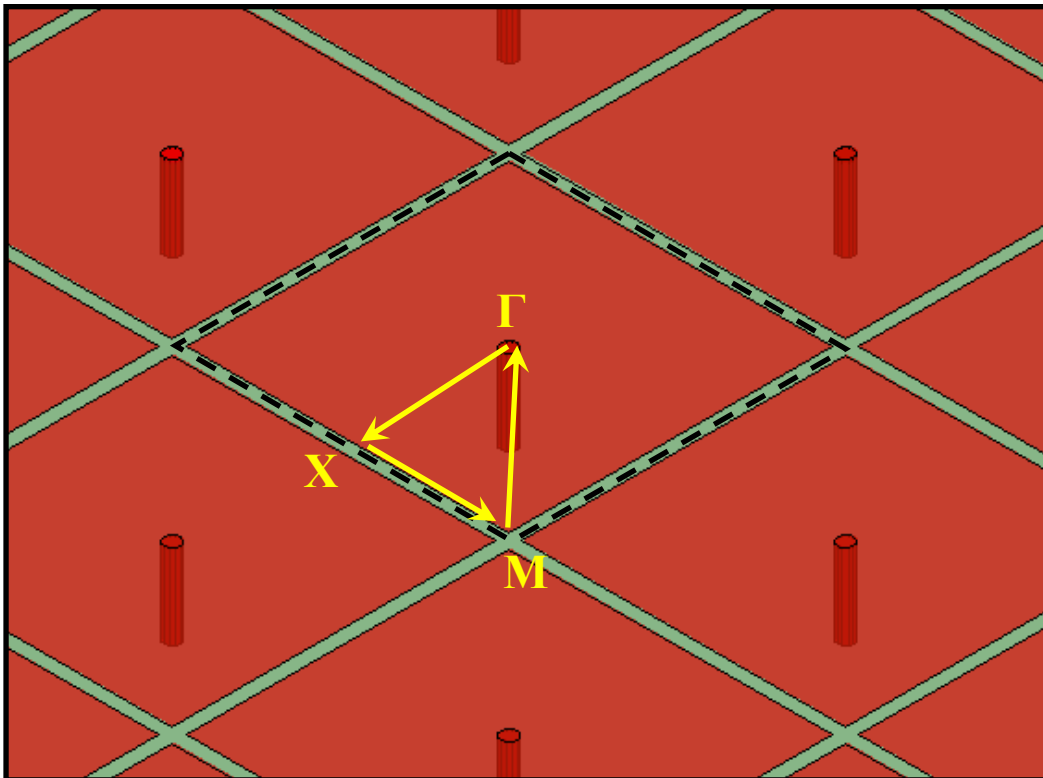


# Sievenpiper Unit-Cell: Driven Mode

1-D dispersion diagram (from Port 1 to Port 2)



# Eigenmode Solver: 2-D Dispersion Diagram



**Γ to X**:  $px=0^\circ, py=0^\circ \rightarrow 180^\circ$

**X to M**:  $px=0^\circ \rightarrow 180^\circ, py=180^\circ$

**M to Γ** :  $px, py: 0^\circ \rightarrow 180^\circ$

- $px$ : phase offset in x-direction
- $py$ : phase offset in y-direction

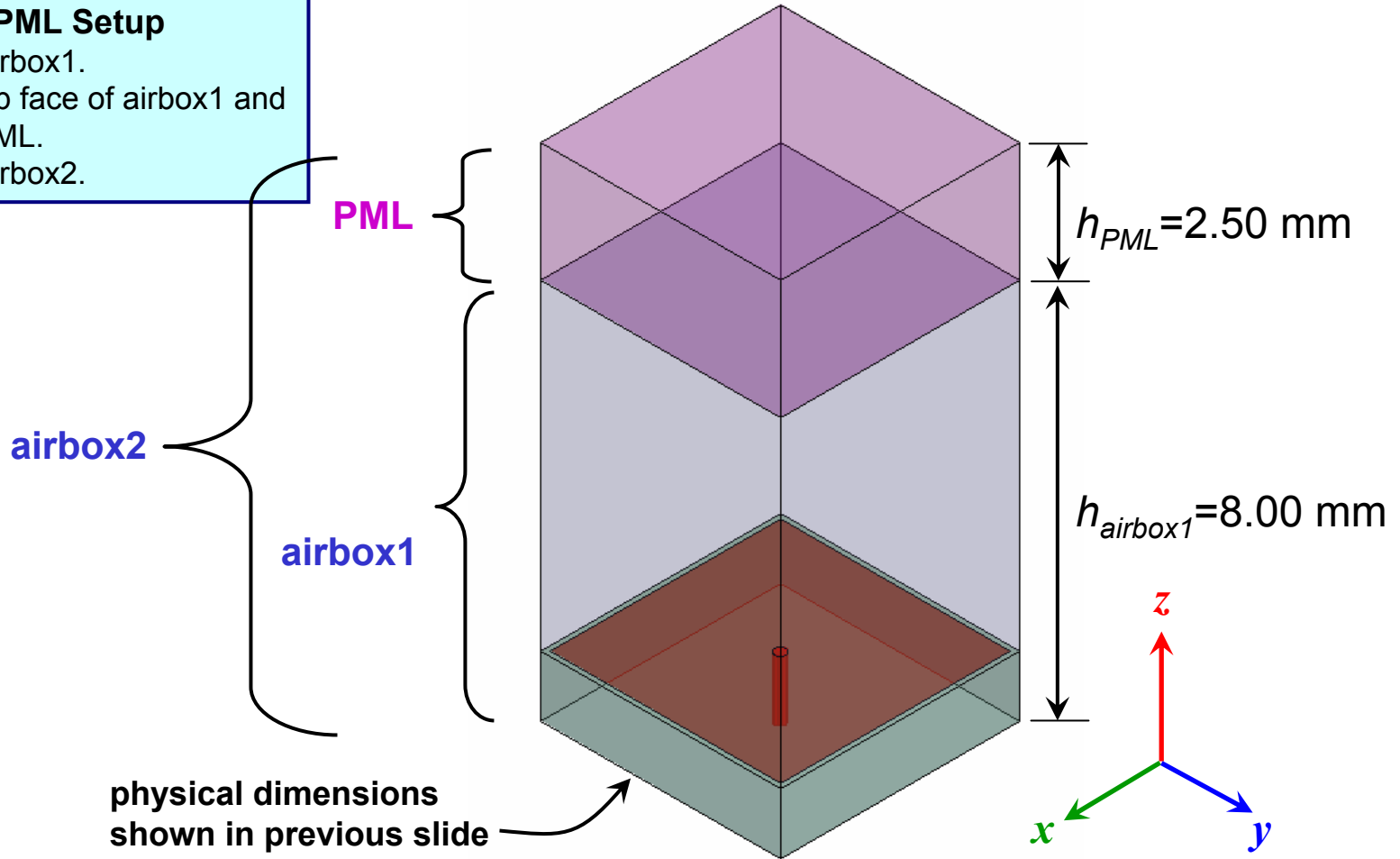
Use Linked Boundary Conditions (LBCs) in HFSS to apply required phase shifts.



# Sievenpiper Unit-Cell Setup

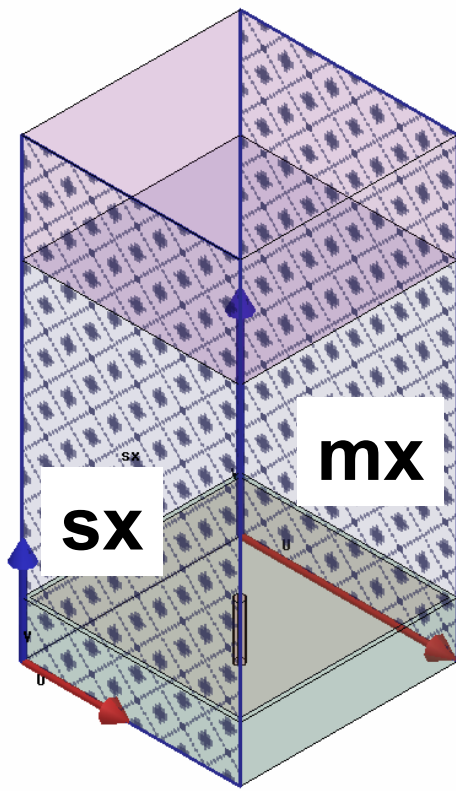
## Airbox and PML Setup

1. Create airbox1.
2. Select top face of airbox1 and assign PML.
3. Create airbox2.



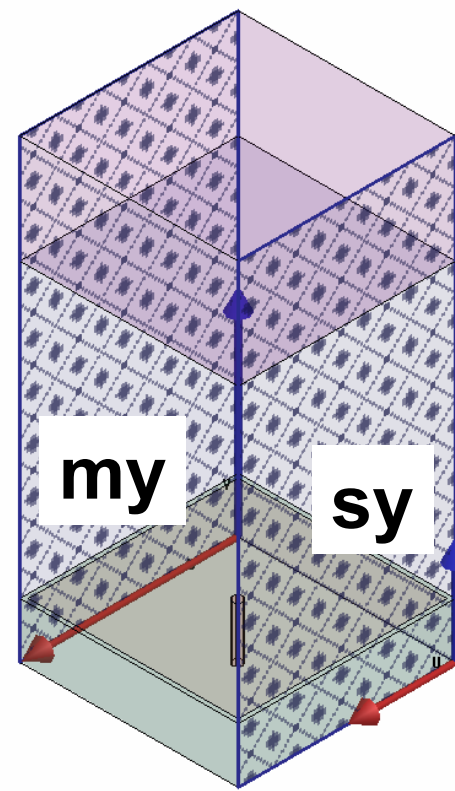
# Unit-Cell Setup: Linked Boundaries

XZ - Planes



- phase delay: px (180 deg)

YZ - Planes

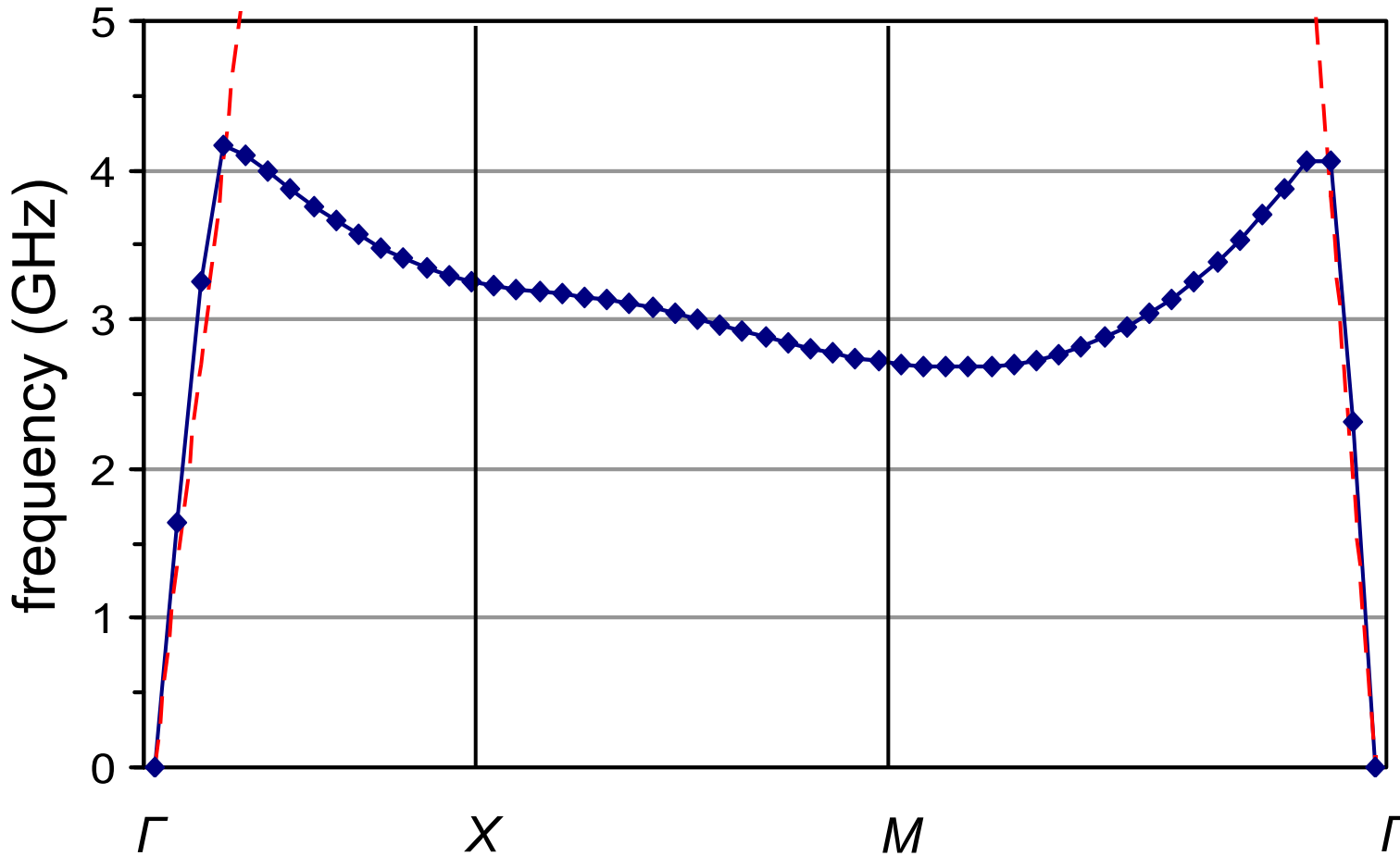


- phase delay: py (0 deg)

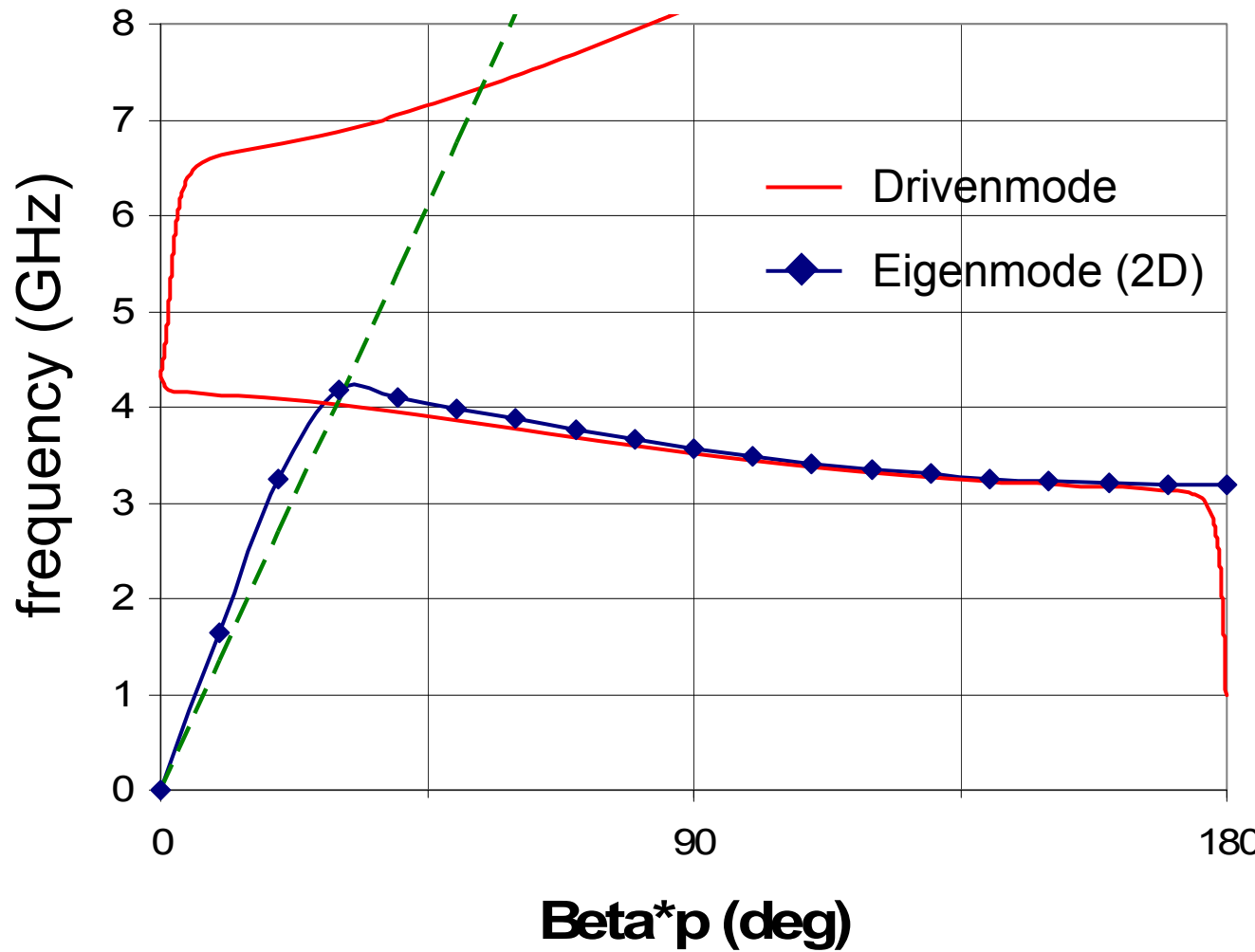


# Eigenmode 2-D Dispersion Diagram

Plotted in Microsoft Excel



# Dispersion Comparison: 1-D vs 2-D Solve

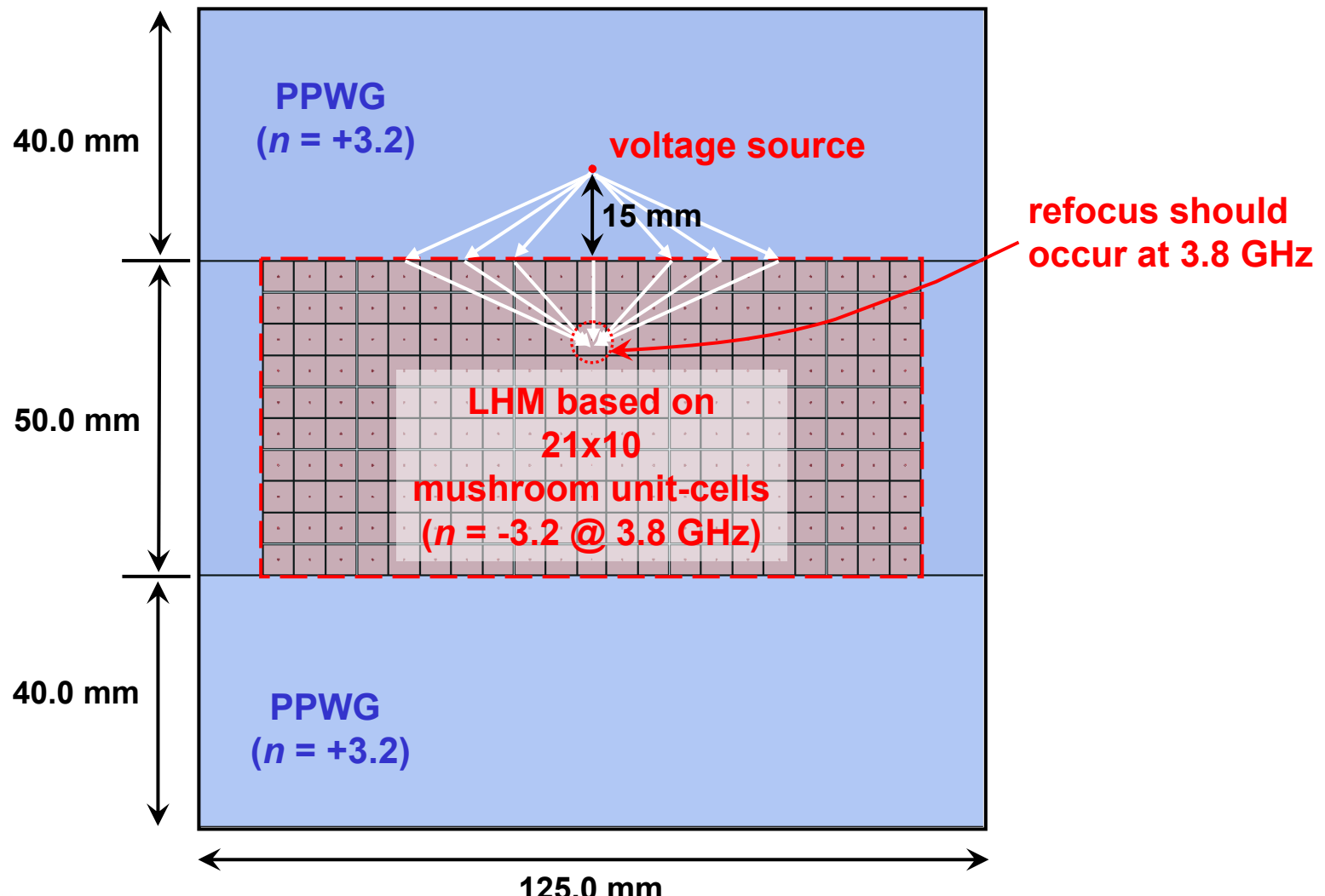


Use drivenmode to quickly characterize/design, eigenmode to verify

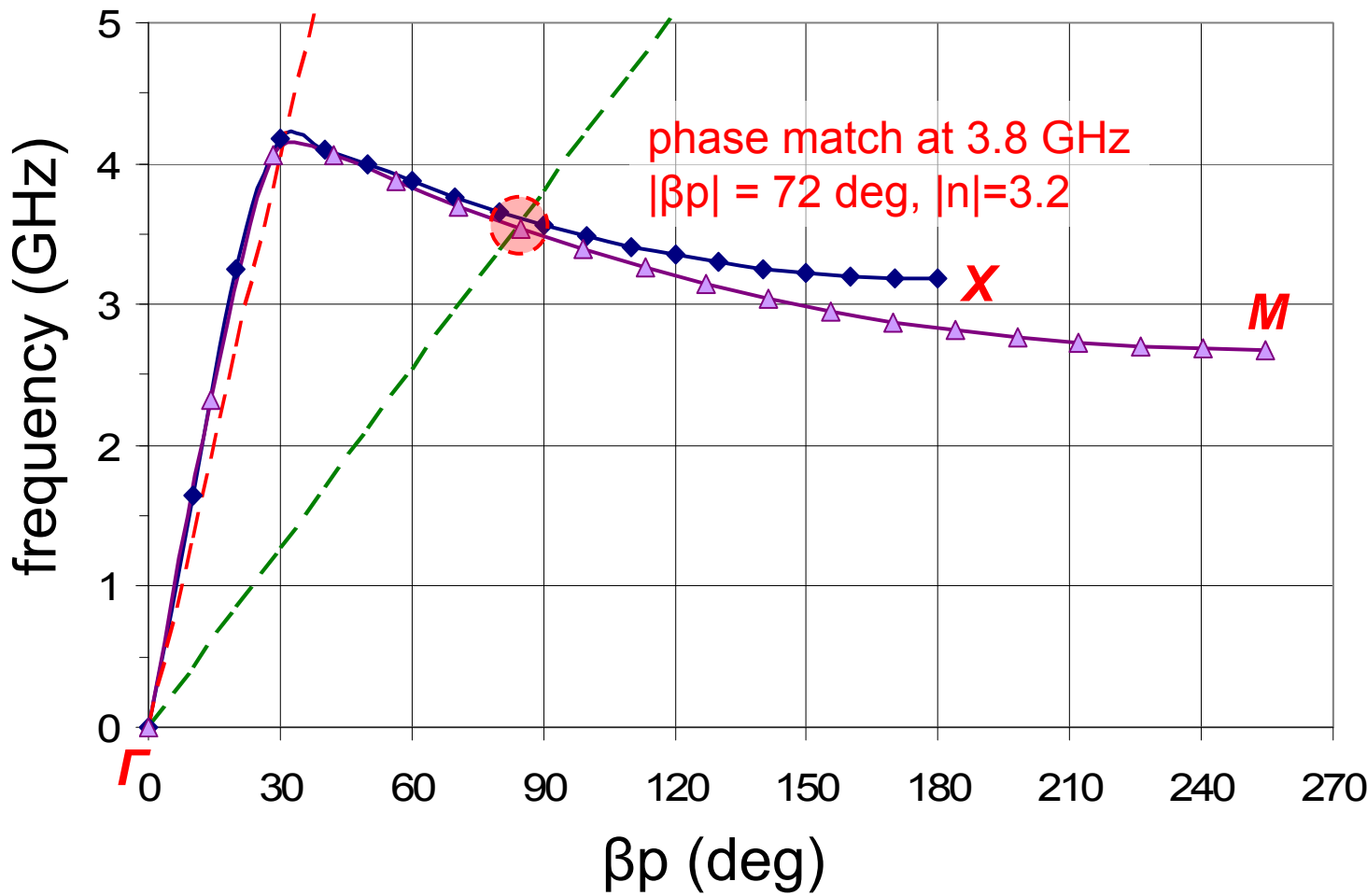


# Flat Lens – Physical Realization

Entire circuit on Roger RT 6010 substrate with  $\epsilon_r = 10.2$  and  $h = 1.27\text{mm}$

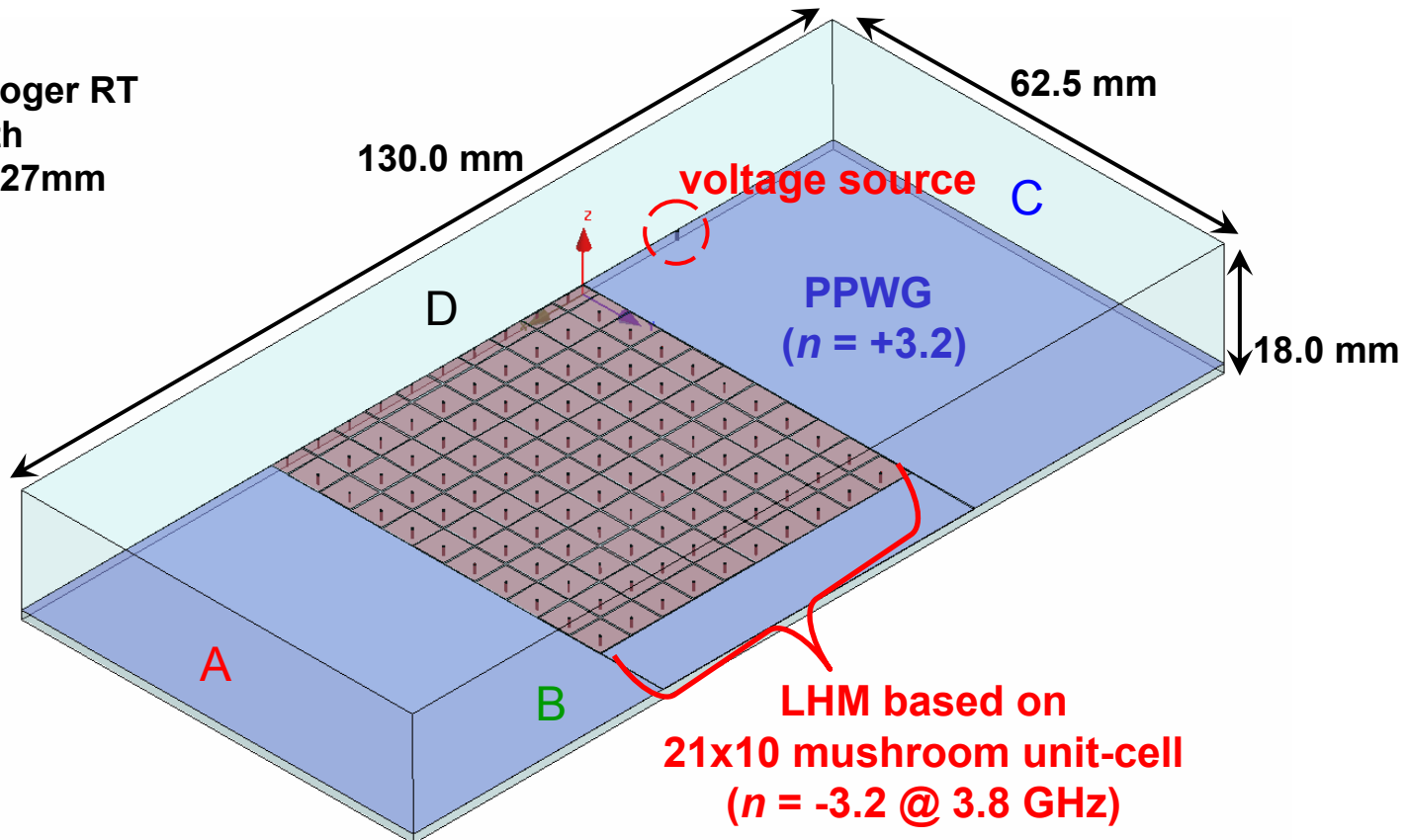


# Flat Lens – Phase Matching Condition



# Flat Lens – Simulation Setup

Entire circuit on Roger RT  
6010 substrate with  
 $\epsilon_r = 10.2$  and  $h = 1.27\text{mm}$



## Boundary Conditions

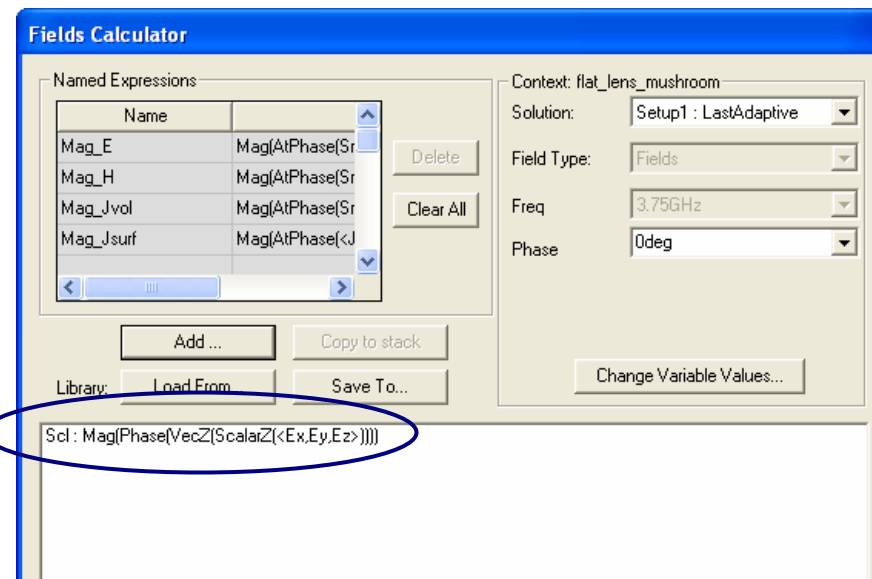
- Radiation boundary applied on Top and Side A, B, and C of air box.
- Finite conductivity (Copper) applied on bottom of airbox, PPWG trace, and mushroom patches.
- Symmetry boundary (perfect-H) applied to Side D to reduce problem size.



# Flat Lens – Field Calculator for Phase

To plot the E-field phase, the field calculator has to be used.

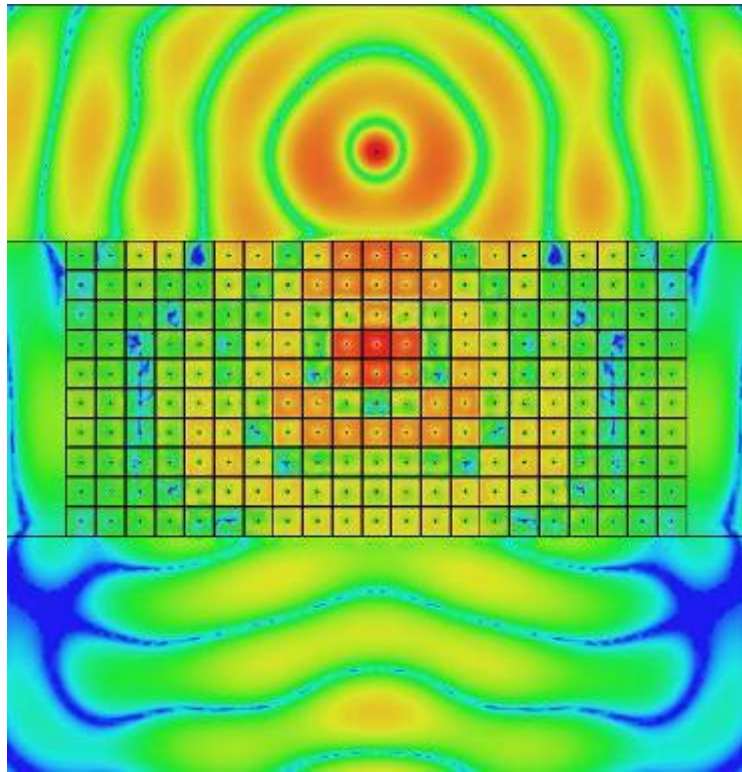
- Go to *HFSS > Fields > Calculator*
- Since the field is quasi-TEM, only the z-component of the E-field is required.
  - ❖ Quantity > *E*
  - ❖ Scal? > *ScalarZ*
  - ❖ Vec? > *VecZ*
  - ❖ Complex > *CmplxPhase*
  - ❖ Mag
  - ❖ Add, give name *PhazeZ*



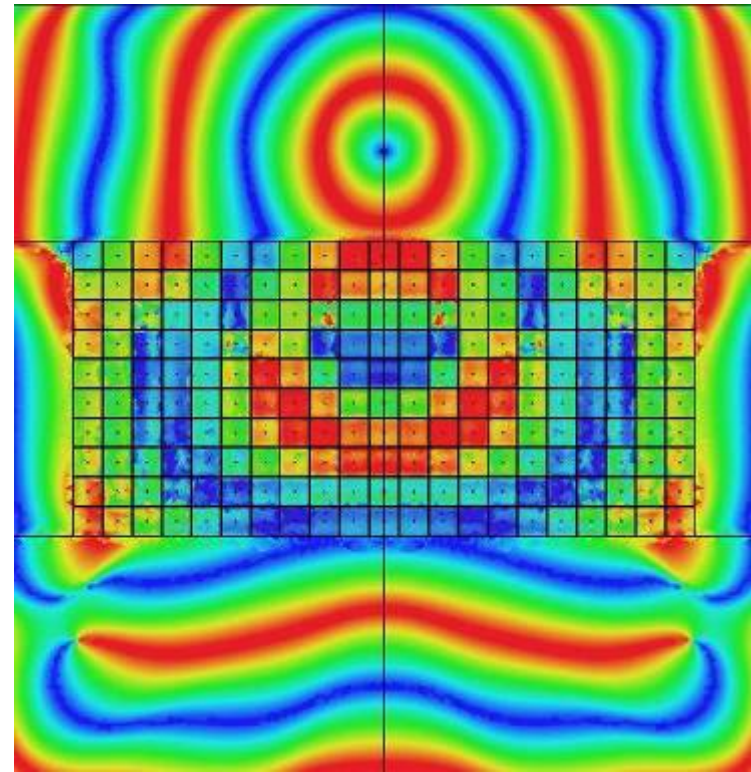
# Flat Lens – E-Field Plots (Ground Plane)

field on ground plane @ f=3.75 GHz

Magnitude



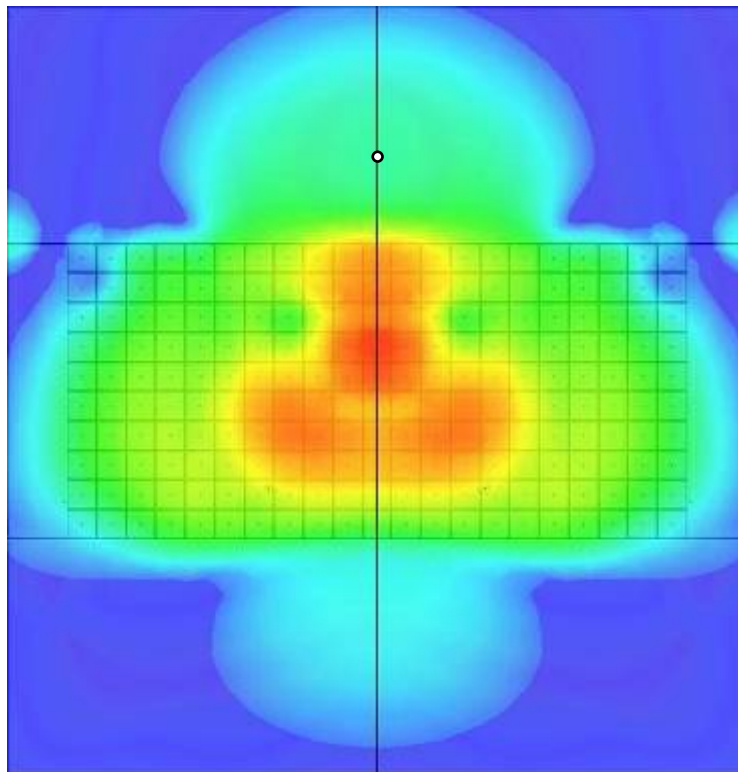
Phase



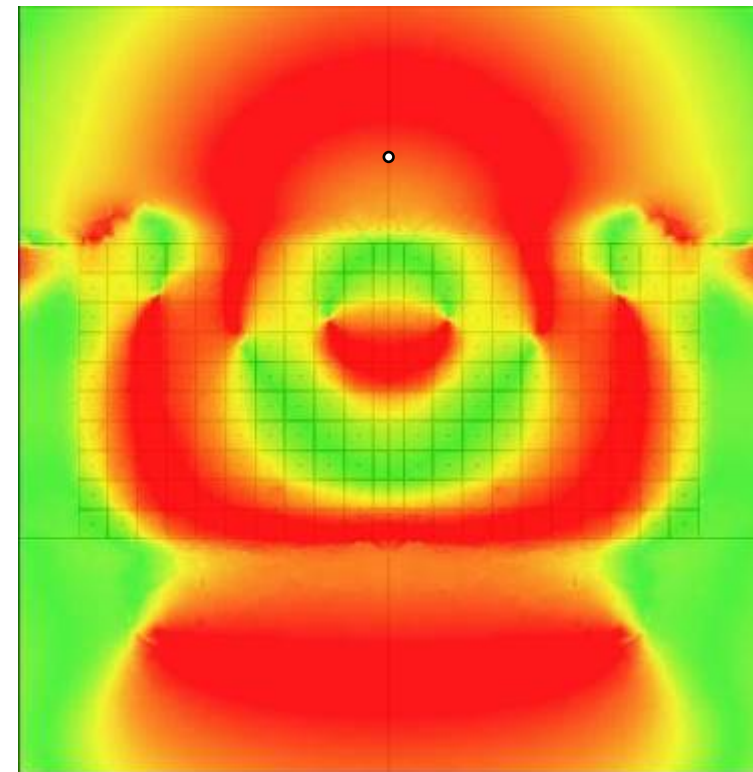
# Flat Lens – E-Field Plots (Above Structure)

field on top of structure @  $f=3.75$  GHz  
(3.5 mm above top metal)

Magnitude

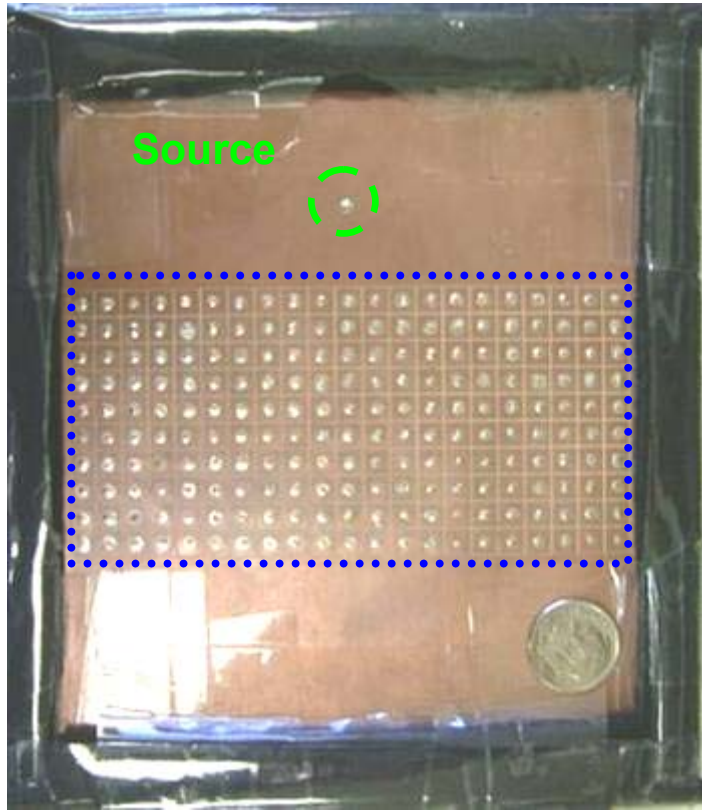


Phase

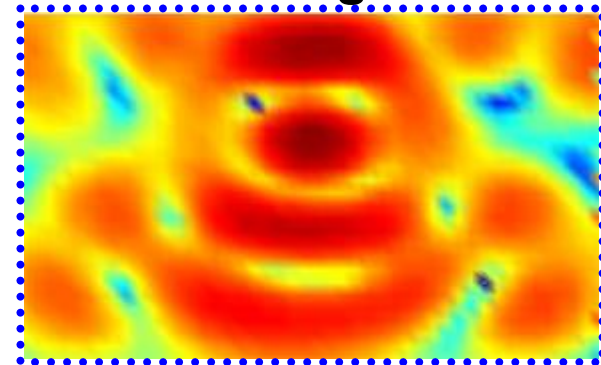


# Flat Lens – Experimental Results

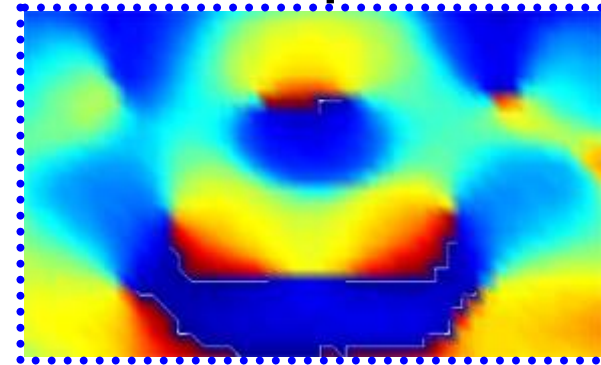
$$f_0 = 3.79 \text{ GHz}$$



E-field magnitude



E-field phase



E-field measured ~ 3.5 mm above

CRLH region



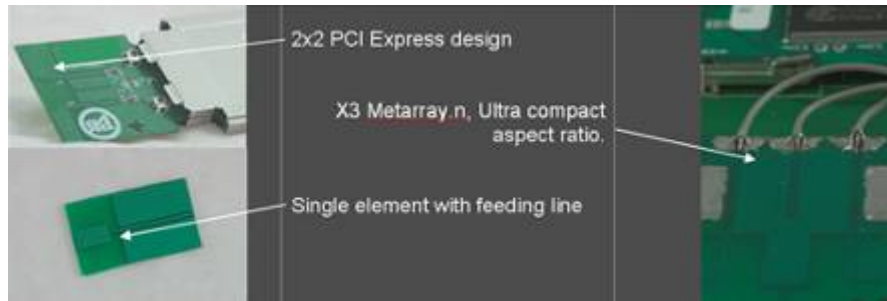
# Future Trends



# Applications & Research

Metamaterial Multiple-Input-Multiple-Output (MIMO)  
Arrays for 802.11n Application [11]

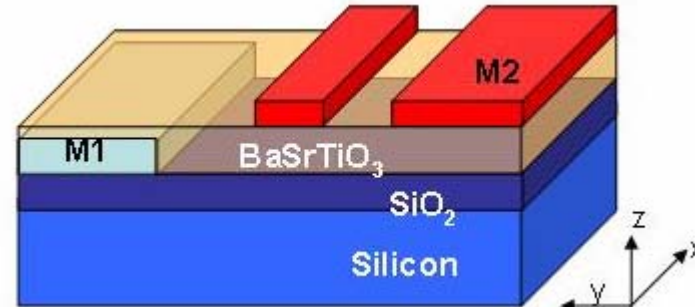
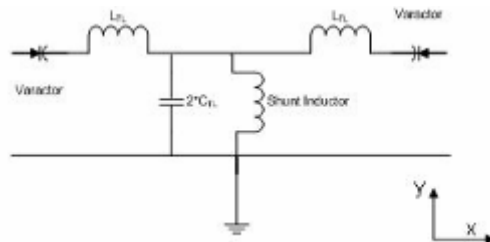
**RAYSPAN™**



## Active CRLH Metamaterials

- High-gain leaky-wave antennas (embed amplifiers in unit-cell) [12]
- Distributed amplifiers [13]

## Tunable Phase Shifters [14]



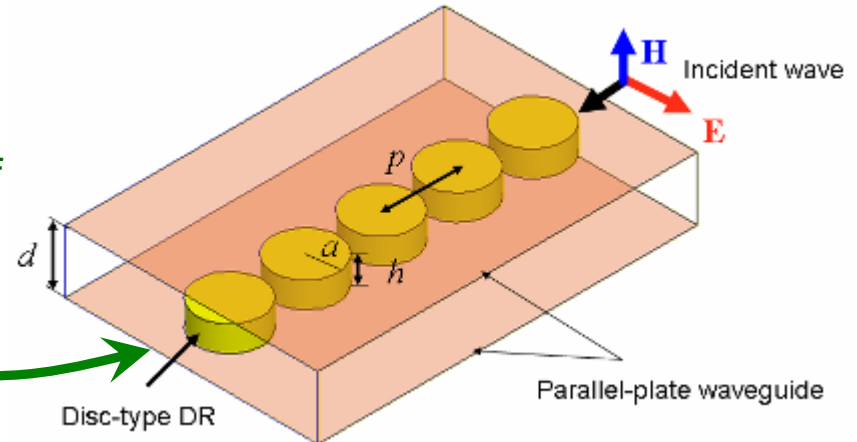
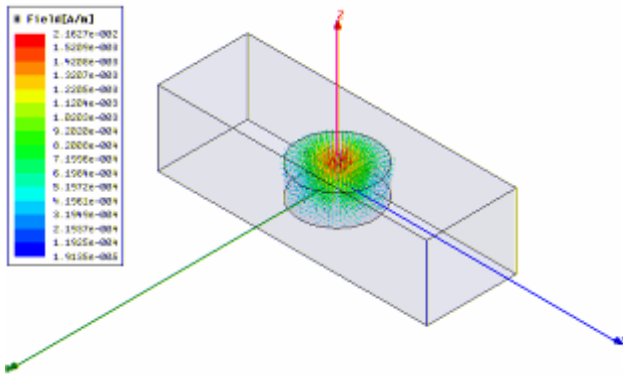
# Implementations

Nano-Metamaterials: optical frequency applications [15]

Evanescence-Mode Metamaterials [16]

1-D LHM: cylindrical DRs in TE mode cutoff  
parallel plate waveguide ( $-\epsilon$ )

H-field Profile (TE<sub>01δ</sub> mode,  $-\mu$ )



Three-Dimensional Metamaterials [17]



# Summary

- Left-Handed Metamaterial Introduction
  - ❖ Resonant approach
  - ❖ Transmission line approach
- Composite Right/Left-Handed Metamaterial
- Metamaterial-Based Microwave Devices
  - ❖ Dominant leaky-wave antenna
  - ❖ Small, resonant backward wave antennas
  - ❖ Dual-band hybrid coupler
  - ❖ Negative refractive index flat lens
- Future Trends



# References

- 1) C. Caloz, C.C. Chang, and T. Itoh, "Full-wave verification of the fundamental properties of left-handed materials (LHMs) in waveguide configurations," *J. App. Phys.*, vol. 90, no. 11, pp. 5483-5486, Dec. 2001.
- 2) R.A. Shelby, D.R. Smith, and S. Schultz, "Experimental verification of a negative index of refraction," *Science*, vol. 292, pp. 77-79, Apr. 2001.
- 3) A. Lai, C. Caloz, and T. Itoh, "Composite right/left-handed transmission line metamaterials," *IEEE Microwave Magazine*, Vol. 5, no. 3, pp. 34-50, Sep. 2004.
- 4) C. Caloz and T. Itoh, *Electromagnetic Metamaterials: Transmission Line Theory and Microwave Applications*, Wiley and IEEE Press, Hoboken, NJ, 2005.
- 5) D. Sievenpiper, L. Zhang, R.F.J. Broas, N.G. Alexopolous, and E. Yablonovitch, "High-impedance surface electromagnetic surfaces with a forbidden frequency band," *IEEE Trans. Microwave Theory Tech.*, vol. 47, no. 11, pp. 2059-2074, Nov. 1999.
- 6) L. Liu, C. Caloz, and T. Itoh, "Dominant mode (DM) leaky-wave antenna with backfire-to-endfire scanning capability," *Electron. Lett.*, vol. 38, no. 23, pp. 1414-1416, Nov. 2002.
- 7) C.J. Lee, K.M.K.H. Leong, and T. Itoh, "Design of resonant small antenna using composite right/left-handed transmission line," *Proc. IEEE Antennas and Propagation Society Int. Symp.*, Washington D.C., Jun. 2005.
- 8) A. Lai, K.M.K.H. Leong, and T. Itoh, "Infinite wavelength resonant antennas with monopolar radiation patterns based on periodic structures," *IEEE Trans. Antennas Propag.*, vol. 55, no. 3, pp. 868-876, Mar. 2007.
- 9) I. Lin, C. Caloz, and T. Itoh, "A branch-line coupler with two arbitrary operating frequencies using left-handed transmission lines," *IEEE-MTT Int. Symp. Dig.*, Philadelphia, PA, Jun. 2003, vol. 1, pp. 325-327.
- 10) A. Lai, "Theory and design of composite right/left-handed metamaterial-based microwave lenses," Master Thesis, Dept. E. E., UCLA, Los Angeles, CA, 2005.
- 11) Rayspan Corporation, <http://www.rayspan.com>
- 12) F. P. Casares-Miranda, C. Camacho Peñalosa, and C. Caloz, "High-gain active composite right/left-handed leaky-wave antenna," *IEEE Trans. Antennas Propag.*, vol. 54, no. 8, pp. 2292-2300, Aug. 2006.
- 13) J. Mata-Conteras, T. M. Martin-Guerrero, and C. Camacho-Peñalosa, "Distributed amplifiers with composite right/left-handed transmission lines," *Microwave Opt. Technol. Lett.*, vol. 48, no. 3, pp. 609-613, March 2006.
- 14) E.S. Ash, "Continuous phase shifter using ferroelectric varactors and composite right-left handed transmission lines," Master Thesis, Dept. E.E., UCLA, Los Angeles, CA 2006.
- 15) V.A. Podolskiy, A.K. Sarychev, and V.M. Shalaev, "Plasmon modes in metal nanowires and left-handed materials," *J. Nonlin. Opt. Phys. Mat.*, vol. 11, no. 1, pp. 65-74, 2002.
- 16) T. Ueda, A. Lai, and T. Itoh, "Demonstration of negative refraction in a cutoff parallel-plate waveguide loaded with 2-D square lattice of dielectric resonators," *IEEE Trans. Microwave Theory Tech.*, vol. 55, no. 6, pp. 1280-1287, Jun. 2007.
- 17) M. Zedler, P. Russer, and C. Caloz, "Circuital and experimental demonstration of a 3D isotropic LH metamaterial based on the rotated TLM scheme," *IEEE-MTT Int'l Symp.*, Honolulu, HI, Jun. 2007.



# Design Guide

- Ansoft Designer: 1-D Leaky-Wave Antenna

## • Ansoft HFSS: Negative Refractive Index Flat Lens

## Chapter 3

# Ansoft HFSS: Negative Refractive Flat Lens

The fundamental background was supported by the COMSOL software, is used to realize a flat negative refractive index (NRI) lens. Ansoft HFSS is used to generate the three-dimensional dispersion diagram for the two-dimensional lens unit cell. In addition, design rules and a driver script are presented to quickly design and analyze a two-dimensional negative refractive lens. The matching condition for realizing a flat NRI lens is also presented. Magnitude and phase field plots in HFSS are used to confirm the negative refractive coating within the COMSOL numerical lens.

### 3.1 Introduction

One of the unique features of left-handed metamaterials that Veselago discussed in his research paper [1] is a negative index of refraction,  $n$ . Therefore, in the special case when both  $n$  and  $\mu$  are negative, it is defined as

$$n = \sqrt{1 - (\epsilon_r - \mu_r)} = -\sqrt{\epsilon_r \mu_r}. \quad (3.1)$$

With the definition of refractive index from (3.1), Snell's law is modified to

$$k_{\text{refr}} = \sin^{-1}\left(\frac{n_{\text{refr}}}{n_{\text{air}}}\sin k_{\text{air}}\right). \quad (3.2)$$

Fig. 3.1 shows the localized application of (3.2) at a RH/LH interface. In the particular case that

$$|n_{\text{air}}| = |\sqrt{\epsilon_{\text{air}}/\mu_{\text{air}}}| = |\epsilon_{\text{air}}| = |\sqrt{\epsilon_{\text{air}}/\mu_{\text{air}}}|, \quad (3.3)$$

no reflection occurs at the RH/LH boundary and  $k_{\text{refr}}$ , which is not possible with a RH/RH interface, depends on dielectric parameters.

Generally, Veselago pointed that a lens could not be realized by using LH materials. In particular, he stated that LH material-based lenses would be the dual of conventional (i.e. RH) lenses.

...the convex and concave lenses have "diverged phases," since the convex lens has a diverging effect and the concave lens is converging effect [1].

34

(a) 59  
(b) 47  
3.20 3.00 2.80  
(c) 40  
(d) 21